J. Mech. Phys. Solids 193 (2024) 105885

Contents lists available at ScienceDirect

Journal of the Mechanics and Physics of Solids

journal homepage: www.elsevier.com/locate/jmps

Energetic exhaustiveness for the direct characterization of energy forms of hyperelastic isotropic materials

Federico Oyedeji Falope [a,b,c,*], Luca Lanzoni [a,c], Angelo Marcello Tarantino [a,c]

[a] DIEF, Department of Engineering "Enzo Ferrari", via P. Vivarelli 10, 41125 Modena, Italy
[b] National Group of Mathematical Physics (GNFM-INdAM), FIM UNIMORE, Via G. Campi, 213/A, 41125 Modena, Italy
[c] CRICT, Centro di Ricerca Interdipartimentale Costruzioni e del Territorio, via P. Vivarelli 10, 41125 Modena, Italy

ARTICLE INFO

Keywords:
Direct methodology
Determination of response functions
Energetic exhaustiveness
Isotropic hyperelastic material
Constitutive inequalities
Violation of empirical inequalities
Biaxial test
Rubber-like materials

ABSTRACT

It is common practice to characterize the constitutive law of a material indirectly. This takes place by fitting a specific stress component, which is given as a combination of response functions or derivatives of the energy function of the material. Yet, it is possible to characterize each energy derivative of the material directly. Not only that but, through a few well-designed tests, getting a set of well-distributed data that defines the evolution of the energy derivatives in the invariant space is attainable, but not for all tests. Here, each test is portrayed as an equilibrium path on the surfaces (or volumes) of the derivative of the energy function. In the framework of the homothetic tests of hyperelastic isotropic materials, we propose the definition of *energetic exhaustiveness*. This definition relates to the capability of a test, via its analytic formulation according to a proper set of deformation invariants, to directly provide a closed-form solution for the derivatives of the energy function. In reaching this definition and retracing the Baker–Ericksen and the empirical inequalities, an alternative form of Baker–Ericksen inequalities is presented. We demonstrate that the unequal-biaxial test alone is energetically exhaustive and that it can provide (the same and more) information on the energy compared to the uniaxial, equi-biaxial, and pure shear tests. Unequal-biaxial experiments on three rubbers are presented. The outcomes of experiments contradict the empirical inequalities and seem to suggest new hierarchical empirical inequalities. Compact and nearly exact solutions are provided to perform and design tests at a constant magnitude of distortion, thus reaching a direct and comprehensive representation of the energy.

1. Introduction

Rubber-like materials and soft tissues reveal an extremely marked non-linear response when undergo large deformations. To comprehend the mechanics of this behaviour, it is necessary to abandon the *ut tensio, sic vis* Hookean approach (Hooke, 1678). An already known problem to the founding fathers of mechanics of non-linear elasticity was the choice of the elastic potential (Ariano, 1925, 1929; Signorini, 1930, 1959; Truesdell and Noll, 1966).[1] The choice of the functional form of the elastic energy W first

* Corresponding author at: DIEF, Department of Engineering "Enzo Ferrari", via P. Vivarelli 10, 41125 Modena, Italy.
E-mail address: federicooyedeji.falope@unimore.it (F.O. Falope).

[1] Ariano (1929) regarding the energy function (or internal potential), observed "*In altri termini con tale nome intendiamo denotare una funzione che esprime l'attitudine complessiva del sistema a produrre lavoro, vale a dire la sua totale energia potenziale, intesa non solo nel senso meccanico, ma anche nel senso elettrico, magnetico, ecc., e quindi l'eguaglianza sopraccennata non è che una diretta conseguenza del principio di conservazione dell'energia*".

Signorini (1959) on pg.2 opened one of his collections stating "*È quindi duplice anche la difficoltà di estendere la Elasto meccanica oltre i suoi confini abituali. Rinunziando a trattare gli spostamenti elastici come spostamenti infinitesimi, si va incontro a problemi al contorno di tipo non lineare, e, quasi ciò non bastasse, prima di ogni calcolo numerico si ha da affrontare un problema estremamente difficile di vera Fisica Matematica: scelta dell'espressione completa del potenziale elastico*".

Truesdell (1956) referred to the choice of the elastic energy as the "*Hauptproblem*".

To date, the definition of the energy form of a material is still a rational fashion an open topic (Saccomandi and Vianello, 2024; Saccomandi, 2024).

https://doi.org/10.1016/j.jmps.2024.105885
Received 17 April 2024; Received in revised form 19 September 2024; Accepted 26 September 2024
Available online 1 October 2024

requires the acceptance of an appropriate representation form. Rivlin and Ericksen (1955) formulated the representation theorem for an isotropic tensor function of a generic coaxial and isomorphic tensor. The choice of the generic tensor confers the measure of deformation chosen for the representation. Among the first representations of the energy, $W = W(\mathbf{C})$, where $\mathbf{C} = \mathbf{F}^{\mathrm{T}}\mathbf{F}$ is the right Cauchy–Green deformation tensor, remains one of the most commonly used constitutive laws. It is the closure equation providing a bridge between kinematics and mechanics.

Before the representation theorems, constitutive law was commonly represented as a stress measure given as the work conjugate of a deformation measure. For instance, using the chain rule, it can be expressed in terms of the first Piola–Kirchhoff stress tensor as $\mathbf{T}_{\mathrm{R}} = \partial W/\partial \mathbf{F} = 2\mathbf{F}\,\partial W/\partial \mathbf{C}$ in the case of isotropic materials. The representation theorem makes it natural to introduce the material response functions as an alternative form of constitutive law (Truesdell, 1952; Truesdell and Noll, 1966; Blatz and Ko, 1962; Beatty, 1987). Response functions depend on the invariants of the deformation measure and the associated *derivatives of the energy function* (DEF).

The importance of establishing restrictions (inequalities) for response functions or DEF was clear immediately. The term *constitutive inequalities* was coined to indicate analytic constraints on combinations of DEF and kinematic amounts. Insights and limitations on constitutive parameters or functional forms of the energy function were also found investigating the existence of the elastic potential, its convexity, and symmetry (Ball, 1976; Ciarlet, 1988; Lainé et al., 1999). Among the first works on constitutive inequalities, two were the main goals: to provide a proper mathematical bound on response function or DEF (Truesdell, 1952; Baker and Ericksen, 1954; Coleman and Noll, 1959; Truesdell and Noll, 1966; Batra, 1976); and to establish the most appropriate measure of deformation (conjugated variable) to reproduce the isotropic response functions (Hill, 1968, 1970; Ogden, 1970, 1977). Noteworthy is also the concept of isotropic constraint (see Carroll, 2009). Among these researches, the work of Baker and Ericksen (1954) has undoubtedly introduced an important and compact constraints known as Baker–Ericksen (*BE*)-inequalities.

Representation theorems and inequalities involving energy, via fitting of experimental tests, primarily aim to grasp and reproduce the mechanical behaviour of the materials. Starting from constitutive inequalities, experiments on rubber-like materials (Rivlin and Ericksen, 1955; Blatz and Ko, 1962) were exploited to propose new inequalities by restricting the existing ones. These were named *empirical* (*E*)-inequalities and were discussed by Truesdell and Noll (1966) as a particular restriction of the *BE*-inequalities. However, *E*-inequalities should not be charged with Truesdell and Noll (1966) (Thiel et al. (2019)) since the authors argued about them as a *mere conjecture*. Indeed, it has been realized that certain things do not fit within *E*-inequalities, leading to the proposal of the *generalized empirical inequalities* (Mihai and Goriely, 2011, 2013).

The reasoning of these works has largely depended on utilizing limitations of DEF to characterize a specific behaviour of a material which is subject to precise testing. The "specific" attribute of the mechanical behaviour recalls that it is a combination of DEF. At most, the energy function of the materials was investigated by the *simultaneous fitting* (Anssari-Benam and Horgan, 2022; Falope et al., 2024) of different tests referred to stress components associated with each test. This approach can be overcome by directly characterizing the DEF of a material. However, this is not permitted by all measures of deformation used to formulate the boundary value problem of isotropic materials, even by any experimental test.

In the wake of this approach, the Mooney function, which combines DEF approached in the invariants of $\mathbf{C}$, was used to carry out the fitting procedure of experiments and gain insights on the shape of the energy function (Rivlin and Ericksen, 1955; Gent and Thomas, 1958; Destrade et al., 2017). However, although it works and is well suited to the purpose required, a great limitation of this approach emerges since it provides information only regarding combinations of DEF. This approach does not optimize experiments for a description of the energy. Nevertheless, it can provide highly accurate results by choosing suitable interpolating functions and proper physical conditions (Dal et al., 2023; Tikenoğulları et al., 2023). A new emerging formulation (Criscione et al., 2000; Prasad and Kannan, 2020) conceived on a new set of invariants of the Hencky strain is better suited to the direct identification of DEF. However, for certain types of tests, even this formulation cannot offer complete (or *exhaustive*) information on DEF.

Direct characterization of the DEF can be carried out by carefully considering the appropriate choice of the deformation measure and the analytic form of the boundary value problem (BVP) associated with a test. This embraces the definitions of *energetic exhaustiveness* given in this paper, for which only one type of test is sufficient to characterize the DEF of a material. In this regard, the Hencky strain has a marked compatibility with the kinematics of isotropic materials (Ogden, 1970). Information of DEF can be significantly increased using the Hencky strain and its Lode invariants (Criscione et al., 2000; Criscione, 2004; Prasad and Kannan, 2020; Kulwant et al., 2023).

The current work fits into a context in which it is crucial to establish objectively what the real purpose of the characterization of a material is. If the target is the energy form, is there a more suitable test for the determination of DEF than another? The definition of energy exhaustiveness and its corollaries on homothetic tests (or deformations) sublimate the purpose of the work. We show that unequal-biaxial tests alone can provide any information on DEF. This point of view, which considers the DEF as the unknowns of the analytic formulation, avoids the problem of simultaneous fitting and reveals one of the origins of the problem of the existence of several sets of optimal constitutive parameters (Ogden et al., 2004).

The flow chart of Fig. 1 describes the structure of the present work. Section 2 (left block of the flow chart) formulates the problem of hyperelastic isotropic solids subjected to homothetic tests (uniaxial, biaxial, and triaxial tests). Then, we recall the *BE* and *E*-inequalities and propose an alternative form of *BE*-inequalities that emerge from the analytic formulation of the uniaxial and equi-biaxial tests. This is the preamble to look at the BVP considering the DEF as the unknowns of the problem (right block of the flow chart) by which the definition of energetic exhaustive test is introduced. Four relevant corollaries of the Rouché–Capelli theorem follow from the energetic exhaustiveness. These corollaries are considered by investigating two reference measures of deformation. The Cauchy–Green deformation tensor and the Hencky strain tensor are analysed as reference measures of deformation, respectively associated with the DEF W_i and W_{K_i}.

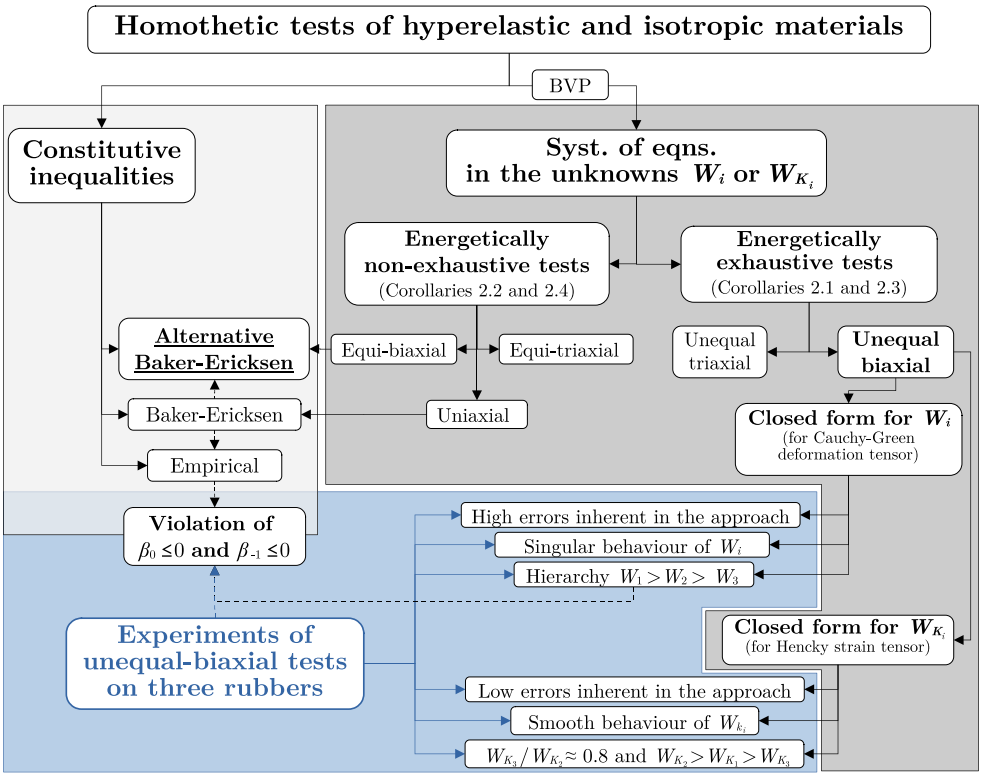

Fig. 1. Graphical representation of the work: constitutive inequalities of isotropic materials (block on the left); analytic formulation of the problem of homothetic deformations (block on the right) approached in the unknowns derivative of the energy function investigated in terms of Cauchy–Green deformation tensor and Hencky strain tensor, $W_i = \partial W/\partial I_i$ or $W_{K_i} = \partial W/\partial K_i$ respectively; experiments of unequal-biaxial tension carried out on three different rubbers (lower blue block).

Experiments on unequal-biaxial test (Appendix B) along with uniaxial tests (Appendix C) are carried out on three different types of rubber-like materials (lower block of the flow chart of Fig. 1). The experimental behaviours of DEF are discussed in Section 3 for both compressible and incompressible materials. Using the closed form solution of DEF, the experiments contradict the E-inequalities. Introducing the incompressibility condition, supported by the experiments, the equilibrium paths on the surfaces of the DEF are discussed for the tested materials. We do not consider the present work as the appropriate forum for a detailed examination of the fitting procedure. Our point of view proposes and examines a rational way to create the best scenario and then proceed via a direct characterization of the DEF. In this regard, Section 3.4 presents a simple design formula to perform tests at a constant value of the magnitude of distortion K_2.

2. Analytic formulation

2.1. Preamble

By the representation theorem (Rivlin and Ericksen, 1955), an isotropic and symmetric 3×3 matrix function of $\mathbb{R}$, denoted with $\mathbf{T}$, is a combination of the identity matrix $\mathbf{I}$, a matrix $\mathbf{A}$, and its square $\mathbf{A}^2$,

$$\mathbf{T} = \alpha_0\mathbf{I} + \alpha_1\mathbf{A} + \alpha_2\mathbf{A}^2. \tag{1}$$

The weighting functions α_i of the combination (1) are the *response functions* (Truesdell and Noll, 1966; Beatty, 1987) of $\mathbf{T}$, which depend on eigenvalues of $\mathbf{A}$. Restriction of coaxiality with $\mathbf{T}$ is required to $\mathbf{A}$. If $\mathbf{A}$ is regular, the Cayley–Hamilton theorem provides an equivalent form of (1)

$$\mathbf{T} = \beta_0\mathbf{I} + \beta_1\mathbf{A} + \beta_{-1}\mathbf{A}^{-1}, \tag{2}$$

being also the β_i response functions of tensor $\mathbf{T}$. The relevance of theorems (1) and (2) is straightforward in the framework of mechanics of solids: they provide an alternative form of the constitutive law of isotropic materials, since $\mathbf{T}$ is the Cauchy stress tensor and $\mathbf{A}$ an appropriate kinematic (reference) tensor associated with its measure of deformation.

The choice of the measure of deformation used to formulate a problem can bring, even on the same problem, more or less information in terms of response functions or DEF with respect to the deformation invariants associated with $\mathbf{A}$.

2.2. DEF approached in the Cauchy–Green deformation tensor and constitutive inequalities

Let us assume the left Cauchy–Green deformation tensor $\mathbf{B} = \mathbf{F}\mathbf{F}^{\mathrm{T}}$ as the kinematic reference tensor. The explicit forms of the material response functions stem from theorems (1) or (2) by introducing the constitutive law

$$\mathbf{T} = \frac{2}{J}\frac{\partial W}{\partial \mathbf{B}} = \frac{2}{J} W_i \frac{\partial I_i}{\partial \mathbf{B}}, \tag{3}$$

where $W = W(I_1, I_2, I_3)$ is the isotropic strain energy function of the material, $W_i = \partial W / \partial I_i$ are the DEF, and I_i the invariants of $\mathbf{B}$ ($I_1 = \mathrm{tr}\mathbf{B}$, $I_2 = \mathrm{tr}\mathbf{B}^*$, and $I_3 = \det \mathbf{B} = J^2$).[2] For homogeneous deformations, the eigenvalues of $\mathbf{T}$ can be directly expressed as a combination of the DEF and eigenvalues of $\mathbf{B}$ (Truesdell, 1952)

$$t_i = \frac{2}{\sqrt{I_3}}\left(I_2 W_2 + I_3 W_3 + W_1 \lambda_i^2 - I_3 \lambda_i^{-2}\right) \text{ (no summation)}. \tag{4}$$

From (4), by relations (1) and (2), one has the explicit form of the response functions

$$\beta_0 = \alpha_0 - I_2\alpha_2 = 2I_3^{-\frac{1}{2}}\left(I_2 W_2 + I_3 W_3\right), \quad \beta_1 = \alpha_1 + \alpha_2 I_1 = 2I_3^{-\frac{1}{2}} W_1, \quad \beta_{-1} = I_3\alpha_2 = -2\sqrt{I_3}\, W_2. \tag{5}$$

Response functions univocally characterize the material dependence in the stress representations (1) and (2). Constitutive inequalities are bounds acting on DEF or the response functions, mitigating the wide gamma of admissible forms of the DEF.

2.2.1. The Baker–Ericksen and the empirical inequalities

Looking for the answer of the *necessary and sufficient conditions that* $t_i > t_j$ (of Eq. (4)) *hold whenever* $\lambda_i > \lambda_j$, Baker and Ericksen (1954) found a correspondence between the response functions,

$$\beta_1 > \frac{\beta_{-1}}{\lambda_i^2 \lambda_j^2} \Rightarrow W_1 + \lambda_i^2 W_2 > 0. \tag{6}$$

The *exact* constitutive inequalities (6) are the *BE*-inequalities.[3] They are often overlooked and not considered in the fitting procedures, as the *E*-inequalities are preferred. *E*-inequalities a priori restrict the solution space of the *BE*-inequalities. Truesdell and Noll (1966), on the wake of the experiments of Rivlin and Saunders (1951) and the outcomes of Baker and Ericksen (1954), premising that "*No theoretical motivation has been found for them*" discussed on the *E*-inequalities[4]

$$\beta_0 \le 0, \quad \beta_1 > 0, \quad \beta_{-1} \le 0, \tag{7}$$

but, asserting that "*thus far I have been unable to derive it in general, and I offer it here merely as conjecture*" (p. 182 of Truesdell and Noll, 1966). Thus, using (5) and (7), it follows

$$\left(I_2 W_2 + I_3 W_3\right) \le 0, \quad W_1 > 0, \quad W_2 \ge 0. \tag{8}$$

Among the explicit form of the *E*-inequalities (8), we will show in Section 3.2 that for some materials tested, Eqs. $(8)_1$ and $(8)_3$ are violated.

2.2.2. The closed-form solution for DEF and the energetic exhaustiveness

The Cauchy stress tensor $\mathbf{T}$ is a stress measure of the deformed configuration. In contrast, the first Piola–Kirchhoff (or nominal) stress tensor, $\mathbf{T}_{\mathrm{R}} = \mathbf{T}\mathbf{F}^*$, given as

$$\mathbf{T}_{\mathrm{R}} = \frac{\partial W}{\partial \mathbf{F}} = 2\left[\left(W_1 + I_1 W_2\right)\mathbf{F} - W_2 \mathbf{B}\,\mathbf{F} + I_3 W_3\,\mathbf{F}^{-\mathrm{T}}\right], \tag{9}$$

refers to the undeformed configuration. Because of stress measurement of the experiments of Appendix B, till now on $\mathbf{T}_{\mathrm{R}}$ is considered as a more appropriate reference measure of stress. From (9), homothetic deformations induce homogeneous states of stress. Thus, disregarding body forces, the indefinite equilibrium conditions $\mathrm{Div}(\mathbf{T}_{\mathrm{R}}) = \mathbf{0}$ are trivially fulfilled. The equilibrium problem reduces to the boundary conditions alone.

Let us focus on homothetic states of deformations where, after deformation, angles are preserved: uni-axial, bi-axial, and triaxial states of stress. For such states of deformation, the deformation gradient is diagonal, $\mathbf{F} = \lambda_i \mathbf{e}_i \otimes \mathbf{e}_i$, and the stress tensor (9) too. The boundary conditions ($\mathbf{T}_{\mathrm{R}}\mathbf{e}_i = \mathbf{s}_i$) take the explicit form of the following system:

$$\begin{cases} 2\lambda_1\left[W_1 + \lambda_2^2 W_2 + \lambda_3^2\left(W_2 + \lambda_2^2 W_3\right)\right] = \bar{\bar{s}}_1 \\ 2\lambda_2\left[W_1 + \lambda_1^2 W_2 + \lambda_3^2\left(W_2 + \lambda_1^2 W_3\right)\right] = \bar{\bar{s}}_2 \\ 2\lambda_3\left[W_1 + \lambda_1^2 W_2 + \lambda_2^2\left(W_2 + \lambda_1^2 W_3\right)\right] = \bar{\bar{s}}_3 \end{cases}, \tag{10}$$

[2] $\mathbf{B}^* = \det \mathbf{B}\,\mathbf{B}^{-\mathrm{T}}$ is the cofactor matrix of $\mathbf{B}$ and $J = \det \mathbf{F}$.

[3] Others constitutive inequalities with more articulated and complex forms were given by Coleman and Noll (1959) and Truesdell and Noll (1966).

[4] In the original version, pg. 158 of Truesdell and Noll (1966), symbol ב, that is the *b* letter of the Semitic abjad, was used instead of the nowadays most diffused β.

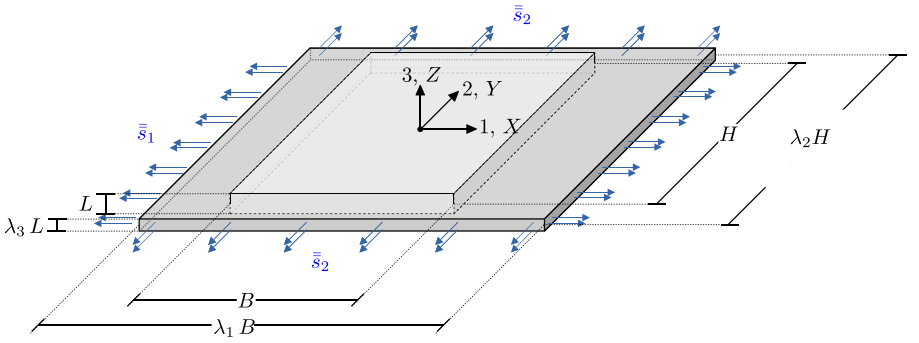

Fig. 2. Reference system for the energetically exhaustive unequal-biaxial test: reference configuration (lighter grey) and deformed configuration (darker grey).

where s_i are the vector components of the surface external nominal pressure (force per unit of undeformed area) while overline symbols $\bar{s}_i$, $\bar{\bar{s}}_i$, and $\bar{\bar{\bar{s}}}_i$ denote the prescribed nominal pressure at boundaries in case of the uniaxial, biaxial or triaxial state of stress, respectively.

Our main concern is the shift of the approach to the system (10), compared to the fitting procedure of the stress, by looking at the DEF as the unknowns of the problem. If we do this, system (10) is a trivial system of algebraic equations,

$$\begin{bmatrix} 2\lambda_1 & 2\lambda_1\lambda_2^2 + 2\lambda_1\lambda_3^2 & 2\lambda_1\lambda_2^2\lambda_3^2 \\ 2\lambda_2 & 2\lambda_2\lambda_1^2 + 2\lambda_2\lambda_3^2 & 2\lambda_1^2\lambda_2\lambda_3^2 \\ 2\lambda_3 & 2\lambda_3\lambda_1^2 + 2\lambda_3\lambda_2^2 & 2\lambda_1^2\lambda_2^2\lambda_3 \end{bmatrix} \begin{bmatrix} W_1 \\ W_2 \\ W_3 \end{bmatrix} = \begin{bmatrix} \bar{\bar{\bar{s}}}_1 \\ \bar{\bar{\bar{s}}}_2 \\ \bar{\bar{\bar{s}}}_3 \end{bmatrix}, \qquad \boldsymbol{\Lambda}\,\boldsymbol{\omega} = \mathbf{s}, \tag{11}$$

in whose matrix form $\boldsymbol{\Lambda}$, $\boldsymbol{\omega}$, and $\mathbf{s}$ are the kinematic coefficient matrix, the unknown vector of DEF, and the vector of applied stress, respectively. It is observed that $\det(\boldsymbol{\Lambda}) = 8\det(\mathbf{F})\prod_{i<j}(\lambda_i^2 - \lambda_j^2)$, with $i \in [1,2]$, $j \in [i+1, 3]$.

Relevant corollaries follow from the application of Rouché–Capelli theorem to homothetic tests (11).

Definition 2.1 (*Energetic Exhaustiveness of a Test*)**.** A test is said *energetically exhaustive* if its matrix form (11) is equivalent to a determined system of equations in the unknowns DEF. A test is said to be *non-exhaustive* if it is equivalent to an undetermined system of equations. A test is said *partially exhaustive* if it provides at least one but not all the DEF independently of each other.

The discriminating character of this definition lies in the matrix representation (11). It depends on the choice of the strain or deformation tensor, its invariants, the representation form, and the test investigated. Two corollaries of the Rouché–Capelli theorem of homothetic tests approached in the invariants I_i of $\mathbf{B}$ follow.

Corollary 2.1. *Unequal-biaxial test and unequal-triaxial test are energetically exhaustive tests since system (11) admits a unique solution,* $\boldsymbol{\omega} \in \mathbb{R}^{3,1}$ *and rank* $\boldsymbol{\Lambda} = rank\,[\boldsymbol{\Lambda}|\,\mathbf{s}] = 3$ ($\lambda_i \neq \lambda_j$ *and* $s_i \neq s_j$).

Corollary 2.2. *Equi-biaxial test and uniaxial test are energetically non-exhaustive tests since system (11) admits* ∞^1 *solutions,* $\boldsymbol{\omega} \in \mathbb{R}^{3,1}$ *and rank* $\boldsymbol{\Lambda} = rank[\boldsymbol{\Lambda}|\,\mathbf{s}] = 2$.[5]

Proposition 2.1. *When formulated in terms of invariants of* $\boldsymbol{B}$*, tests involving homothetic state of deformations can be exhaustive, partially exhaustive*[6] *and non-exhaustive.*

Some homothetic tests, when referred to a specific deformation tensor, do not provide exhaustive information regarding the DEF, as they do not allow for the decoupling of the DEF. The wealth of unequal-triaxial and unequal-biaxial tests is conferred by the triaxial character in terms of deformation. Only the unequal-triaxial test is triaxial also in terms of stress. Each stress varies and the dual stretch too, but differently due to the non-linearity of the constitutive law. Conversely, uniaxial and equi-biaxial (non-exhaustive) tests provide only information regarding combinations of DEF.

[5] For non-exhaustive tests, two eigenvalues coincide: $\lambda_1 = \lambda_2 = \lambda$ and $\bar{s}_1 = \bar{s}_2 = 0$ for uniaxial test; $\lambda_1 = \lambda_2 = \lambda$ and $\bar{\bar{s}}_1 = \bar{\bar{s}}_2 = \bar{\bar{s}}$ for equi-biaxial test. *Corollary* 2.2 outlines one of the main reasons that lead to the indeterminacy of a unique set of constitutive parameters in the fitting problem (see Ogden et al., 2004 for the discussion on the existence of multiple sets of constitutive parameters that can fit the same data).

[6] It is the case of volumetric test (Pelliciari et al., 2023) approached in the modified invariants $\bar{I}_i$ (Ehlers and Eipper, 1998).

Table 1
Combinations of the derivatives of the energy function $W_i = \partial W/\partial I_i$ provided by non-exhaustive tests, approached in the invariants I_i of **B**. The bar and double bar symbols on s denote uniaxial nominal stress and equi-biaxial nominal stress, respectively. Principal stretches $\lambda_1 = \lambda_2 = \lambda$ and λ_3 are referred to the reference system of Fig. 2, where $\bar{s}$ acts along axis 3 and $\bar{\bar{s}}$ in the plane 12. The signs in brackets confirm the Baker–Ericksen inequalities and introduce an alternative form of Baker–Ericksen inequalities.

Non-exhaustive homothetic tests	Information on combinations of W_i	
	Compressible materials	Incompressible materials
Uniaxial test (tension/compression)	$W_2 + \lambda^2 W_3 = -\frac{\bar{s}}{2(\lambda_3^2-\lambda^2)\lambda_3}$ (<0) $W_1 - \lambda^4 W_3 = \frac{\bar{s}}{2(\lambda_3^2-\lambda^2)}\frac{\lambda^2+\lambda_3^2}{\lambda_3}$ (>0) $W_1 + \lambda^2 W_2 = \frac{\bar{s}\,\lambda_3}{2(\lambda_3^2-\lambda^2)}$ (>0)	$\lambda_3 W_1 + W_2 = \frac{\lambda_3^3 \bar{s}}{2(\lambda_3^3-1)}$ (>0)
Equi-biaxial test (tension/compression)	$W_2 + \lambda^2 W_3 = -\frac{\bar{\bar{s}}}{2\lambda(\lambda^2-\lambda_3^2)}$ (<0) $W_1 - \lambda^4 W_3 = \frac{\lambda\bar{\bar{s}}}{(\lambda^2-\lambda_3^2)}$ (>0) $W_1 + \lambda^2 W_2 = \frac{\lambda\bar{\bar{s}}}{2(\lambda^2-\lambda_3^2)}$ (>0)	$W_1 + \lambda^2 W_2 = \frac{\lambda^5\bar{\bar{s}}}{2(\lambda^6-1)}$ (>0)

The closed-form solution of DEF is looked for in the unequal-biaxial test of the solid of Fig. 2. The state of stress is unequal-biaxial ($\bar{\bar{s}}_3 = 0$, $\bar{\bar{s}}_1 > \bar{\bar{s}}_2$), and the state of deformation is triaxial ($\lambda_i \neq \lambda_j$). From equilibrium (11) one has

$$\begin{cases} W_1 = \dfrac{\lambda_1^3\left(\lambda_2^2-\lambda_3^2\right)\bar{\bar{s}}_1 - \lambda_2^3\left(\lambda_1^2-\lambda_3^2\right)\bar{\bar{s}}_2}{2\left(\lambda_1^2-\lambda_2^2\right)\left(\lambda_1^2-\lambda_3^2\right)\left(\lambda_2^2-\lambda_3^2\right)} \\ W_2 = \dfrac{\lambda_1\left(\lambda_3^2-\lambda_2^2\right)\bar{\bar{s}}_1 + \lambda_2\left(\lambda_1^2-\lambda_3^2\right)\bar{\bar{s}}_2}{2\left(\lambda_1^2-\lambda_2^2\right)\left(\lambda_1^2-\lambda_3^2\right)\left(\lambda_2^2-\lambda_3^2\right)} \\ W_3 = \dfrac{\lambda_2\left(\lambda_2^2-\lambda_3^2\right)\bar{\bar{s}}_1 + \lambda_1\left(\lambda_3^2-\lambda_1^2\right)\bar{\bar{s}}_2}{2\lambda_1\lambda_2\left(\lambda_1^2-\lambda_2^2\right)\left(\lambda_1^2-\lambda_3^2\right)\left(\lambda_2^2-\lambda_3^2\right)} \end{cases}. \tag{12}$$

Such expression will be used in Section 3.2 to argue on the experimental behaviour of the DEF for three different types of rubbers. The case of incompressible materials is treated in Appendix A.

2.2.3. Alternative form of BE-inequalities from non-exhaustive homothetic tests

The equilibrium of the non-exhaustive tests of Corollary 2.2 leads to three constitutive inequalities. For uniaxial test and equi-biaxial test, Table 1 explicitly reports the relation between DEF provided by equilibrium (12) of non-exhaustive tests. The reference system of the inequalities is made on Fig. 2, where the uniaxial test develops along direction 3 while the biaxial test works in plane 12. The signs of the inequalities, reported in Table 1 between brackets, are straightforward to check.[7] Fig. 3 summarizes the energetic outcomes on DEF for homothetic tests approached in the invariants of **B**. As a result of Corollary 2.2, uniaxial and equi-biaxial tests provide the same information for the DEF. The last inequality of systems in Table 1 is one of the *BE*-inequalities (6), as well as all the inequalities reported for incompressible materials. The *BE*-inequalities imply the positiveness of the Mooney function (Destrade et al., 2017; Anssari-Benam et al., 2022) $\mathcal{M} = W_1 + W_2/\lambda_3 > 0$. The first two inequalities of the systems in Table 1 are an alternative form of *BE*-inequalities.

2.3. DEF approached in the invariants of the Hencky strain tensor

Let us assume the natural or Hencky strain $\boldsymbol{\eta} = \log \mathbf{V}$ (Fitzgerald, 1980) as kinematic reference tensor, associated with the constitutive law

$$\mathbf{T} = \frac{1}{J}\frac{\partial W}{\partial \boldsymbol{\eta}} = \frac{1}{e^{K_1}}\left(W_{K_1}\mathbf{I} + W_{K_2}\boldsymbol{\Phi} + \frac{W_{K_3}}{K_2}\mathbf{Y}\right). \tag{13}$$

K_i are the invariants of $\boldsymbol{\eta}$ (Criscione et al., 2000; Chen et al., 2012; Kulwant et al., 2023)[8]

$$K_1 = \mathrm{tr}(\boldsymbol{\eta}), \quad K_2 = |\boldsymbol{\eta}^d|, \quad K_3 = 3\sqrt{6}\det(\boldsymbol{\Phi}), \tag{14}$$

[7] Let for instance consider the case of uniaxial tension, for which $\bar{s} > 0$, $\lambda_3 > 1$, and $\lambda_1 = \lambda_2 = \lambda < 1$. The RHS terms of each inequality have a trivially determined sign, and so on for uniaxial compression and biaxial tension/compression.

[8] Symbol $|\mathbf{A}| = \sqrt{\mathbf{A} : \mathbf{A}}$ denotes the magnitude of **A**, $\mathbf{A} : \mathbf{Q} = \mathrm{tr}(\mathbf{A}^{\mathrm{T}}\mathbf{Q})$ is the inner product and the apex d stands for the deviatoric part of **A**.

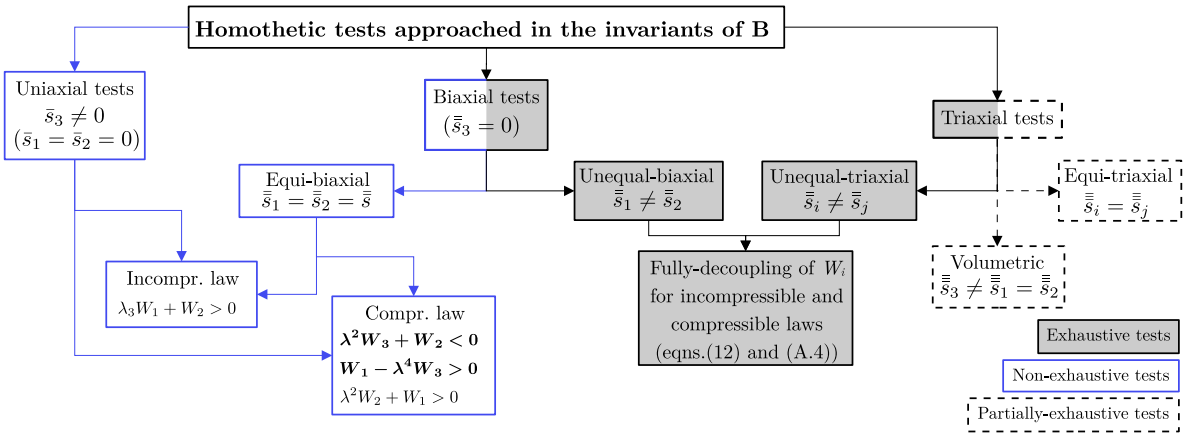

Fig. 3. Graphical representation of the available tests approached in the invariants of **B** with homothetic deformations, subdivided into energetically exhaustive (grey frame), partially exhaustive (dashed frame), and non-exhaustive (blue frame). The exhaustive tests provide a closed-form expression for all the derivatives of the energy function ($W_i = \partial W / \partial I_i$); partially exhaustive tests provide only some derivatives of the energy function; non-exhaustive tests provide only combinations of the derivatives of the energy function. In the case of homothetic tests approached using the invariants of the Hencky strain tensor $\boldsymbol{\eta}$, all non-exhaustive tests become partially exhaustive, Eqs. (12) and (A.4) are replaced by (16) and (A.6), respectively (see Proposition 2.1).

representing respectively the pure volume change, the magnitude of distortion, and the mode of distortion, and terms W_{K_i} are the DEF. The kinematic tensors $\mathbf{Y}$ and $\boldsymbol{\Phi}$ are both deviatoric and coaxial tensors defined as

$$\boldsymbol{\Phi} = \frac{\boldsymbol{\eta}^d}{K_2}, \quad \mathbf{Y} = 3\sqrt{6}\boldsymbol{\Phi}^2 - \sqrt{6}\mathbf{I} - 3K_3\boldsymbol{\Phi}. \tag{15}$$

The representation (13) is a masterpiece of orthogonality. The stress response functions are mutually orthogonal. In addition, $\mathbf{Y} = \mathbf{0}$ in case of uniaxial and equi-biaxial tests.[9] When $\mathbf{Y} = 0$, the closed-form solution for W_{K_3} is lost but, we also lose W_{K_3} as an unknown of the problem. With fewer restrictions than Corollary 2.1 and Corollary 2.2, two corollaries of the Rouché–Capelli theorem of homothetic tests formulated in the invariants K_i of $\boldsymbol{\eta}$ follow.

Corollary 2.3. *Unequal-biaxial test and unequal-triaxial test are energetically exhaustive tests since system (13)[10] admits a unique solution,* $\boldsymbol{\omega} \in \mathbb{R}^{3,1}$ *and rank* $\boldsymbol{\Lambda} = rank\,[\boldsymbol{\Lambda}|\,\mathbf{s}] = 3$ *(*$\lambda_i \neq \lambda_j$ *and* $s_i \neq s_j$*).*

Corollary 2.4. *Equi-biaxial test and uniaxial tests are energetically partially exhaustive since system (13) admits a unique solution:* $\boldsymbol{\omega} \in \mathbb{R}^{2,1}$ *and rank* $\boldsymbol{\Lambda} = rank\,[\boldsymbol{\Lambda}|\,\mathbf{s}] = 2$.

Proposition 2.2. *When formulated in terms of invariants of* $\boldsymbol{\eta}$*, tests involving homothetic state of deformations can be energetically exhaustive or at least partially exhaustive.*

The non-exhaustive tests for the formulation in terms of invariants of **B** become partially exhaustive when formulated in terms of invariants of $\boldsymbol{\eta}$.

In the reference configuration, the equilibrium problem (12) is determined forthwith

$$\begin{cases} W_{K_1} = \dfrac{\bar{\bar{s}}_1\lambda_1 + \bar{\bar{s}}_2\lambda_2}{3} \\ W_{K_2} = -\dfrac{1}{3K_2}\left[\bar{\bar{s}}_1 \log\left(\dfrac{\lambda_2\lambda_3}{\lambda_1^2}\right)\lambda_1 + \bar{\bar{s}}_2 \log\left(\dfrac{\lambda_1\lambda_3}{\lambda_2^2}\right)\lambda_2\right] \\ W_{K_3} = \dfrac{K_2^3}{3\sqrt{6}\log\left(\frac{\lambda_1}{\lambda_2}\right)\log\left(\frac{\lambda_1}{\lambda_3}\right)\log\left(\frac{\lambda_2}{\lambda_3}\right)}\left[\bar{\bar{s}}_1 \log\left(\dfrac{\lambda_2}{\lambda_3}\right)\lambda_1 + \bar{\bar{s}}_2 \log\left(\dfrac{\lambda_3}{\lambda_1}\right)\lambda_2\right] \end{cases}. \tag{16}$$

Relations (12) and (16) embody the equilibrium paths inside the volume of the DEF $W_{K_i} = W_{K_i}(K_1, K_2, K_3)$ or $W_i = W_i(I_1, I_2, I_3)$. For incompressible materials, analogously to (12) and (16), relations (A.4) and (A.6) describe the equilibrium paths, travelled during tests by the material, on the surface of the DEF $W_{I_i} = W_{I_i}(I_1, I_2)$ and $W_{K_i} = W_{K_i}(K_2, K_3)$ respectively.[11]

[9] In case of uniaxial tension (or compression) and equi-biaxial compression (or tension) $K_3 = +1$ (or -1). Such formulation automatically perceives Corollary 2.1 bypassing its undetermined character.

[10] It is referred with the associated BVP $\mathbf{T}_R\mathbf{n}_i = \mathbf{s}_i$.

[11] From equilibrium conditions of equal-biaxial and uniaxial test, *BE*-inequalities become $\text{sign}(\bar{s})\,W_{K_1} \geq 0$ and $W_{K_2} \geq 0$.

3. Experimental evidence and optimization of the outcome of homothetic tests

Before we engage in the discussion on the experimental behaviour of DEF (W_i and W_{K_i}) for compressible and incompressible laws and their consequences, we define how uncertainties related to the DEF are computed.

The uncertainties associated with the instrumentation used in the experiments (of Appendix B and Appendix C) are given in Appendix B.2 (Δ_{DIC}, Δ_{PLO}, and Δ_{cell}). In the quantification of the uncertainties, stretches and stresses are considered independent variables since they are associated with different measurement devices. Conversely, DEF (12), (16), (A.4), and (A.6) are considered functions of the stretches and stresses. The uncertainties of DEF are computed as the propagation rule of a multivariable function,

$$\Delta W_i = \sqrt{\sum_{j=1}^{5} \left(\frac{\partial W_i}{\partial x_j} \Delta x_j \right)^2},$$

being $\boldsymbol{x} = [\lambda_1, \lambda_2, \lambda_3, \bar{\bar{s}}_1, \bar{\bar{s}}_2]$ and $\boldsymbol{\Delta x} = [\Delta_{\text{DIC}}, \Delta_{\text{DIC}}, \Delta_{\text{PLO}}, \Delta_{\text{cell}}, \Delta_{\text{cell}}]$. Covariance between the variables is assumed a priori null. Geometrical uncertainties affecting the specimens are not accounted for. The distribution of stress is assumed constant and the deformations homogeneous. The experiments of Appendix B confirm homogeneous deformations, as the principal directions observed with DIC in Figs. B.13 (d) and (e) are independent of the spatial variable far from the clamping system.

The measurement of all three principal stretches, as required by the compressibility condition of the material, makes each measurable function dependent on three variables. The graphic representation of these functions (stretches, stresses, and DEF) is far from obvious. Differently from the case of incompressible materials (Rivlin and Saunders, 1951; Criscione, 2004; Kulwant et al., 2023), it is not possible to provide iso-invariant plots. Thus, we limit ourselves to plotting these amounts as a function of a most representative invariant. We opt for I_1 and K_2. For incompressible materials, the 2D behaviours of the DEF are provided as a function of both invariants.

3.1. Stretches and stresses

Principal stretches λ_i of the unequal-biaxial test are reported in the first column of Fig. 4 as a function of I_1, while the associated and coaxial nominal stresses are reported in the second column of the figure. The filled regions between the curves of the material delimit the margins of the uncertainty band. Denoted with circular, triangular, and square markers, each test has been repeated three times on the same material. Except for extremely low or high values of deformation, tests show good repeatability.

For stretches and stresses, the negligible uncertainties represent the fitness of the measurement devices (load cells, PLO, and DIC). Along with the curve of λ_3 (measured with PLO), the transversal stretch provided by the incompressibility $\lambda_3 = (\lambda_1\lambda_2)^{-1}$ is reported with a dashed black curve in the first column of Fig. 4. These amounts compare DIC monitoring with the PLO one. For unequal-biaxial tension, the hydrostatic stress is positive so the volume should increase. The experimental value of λ_3 should always lie above the incompressibility curves ($\lambda_3 > 1/\lambda_1\lambda_2$). This is true except for a few values at small deformations and large deformations in the sole para rubber. In silicone specimens, optimal results are reached in terms of kinematics (transversal stretch always lies above the incompressibility curves in Fig. 4) and mechanics, showing extremely narrow margins of uncertainty. Differently from the uniaxial tests of Fig. C.14, silicone is the sole rubber that exhibits hardening in the investigated range of deformation.

3.2. Compressible materials: violation of E-inequalities and DEF singularity

The values of the DEF in the case of compressible materials are shown in Fig. 5. The first column of the figure provides the DEF in terms of invariants of the Cauchy–Green deformation tensor as a function of I_1, while the second column reports DEF in terms of invariants of the Hencky strain as a function of K_2, according to (12) and (16), respectively. In these figures, in addition to I_1 and K_2, the other invariants vary also.

If approached in terms of invariants I_i, the uncertainty is too large at low values of deformation giving rise to a *singular behaviour* of DEF. This singular behaviour is not obvious. It was also observed by Criscione (2004) but interpolating the Jones and Treloar (1975) results. Except for small deformations where the uncertainty dominates, W_1 and W_3 are always positive and negative, respectively. W_2 can be positive, negative, and nearly null for silicone, S-PU and para rubber, respectively Figs. 5(a), (c), and (e). The negative values of W_2 violate the empirical inequalities $(8)_3$. Even with only a single value, Rivlin and Saunders (1951) also found a negative value of W_2. In Table 1 of their work, this value was replaced with the symbol –, probably due to its extremely low magnitude. The E-inequality $(8)_1$ does not mirror the behaviour of silicone rubber. This is shown in Fig. 6(a), where it can be seen that the E-inequality $(8)_1$ of the silicone always assumes positive values.

The silicone tested contradicts the E-inequality $(8)_1$ while the soft polyurethane tested contradicts the E-inequality $(8)_3$. We have tested only three materials, but among these, two materials violated at least one empirical inequality. Having an empirical nature, the violation of the E-inequalities does not invalidate the experiments. On contrary, the experiments invalidate the E-inequalities. Therefore, the E-inequalities are not reliable for these materials. Conversely, the *BE*-inequalities are fully satisfied by the tested materials due to their exact nature.[12]

[12] The *BE*-inequalities in terms of invariant K_i were exploited and argued by Prasad and Kannan (2020) to determine the mathematical form of the shear modulus function and to impose proper boundary conditions on the energy form for brain tissue.

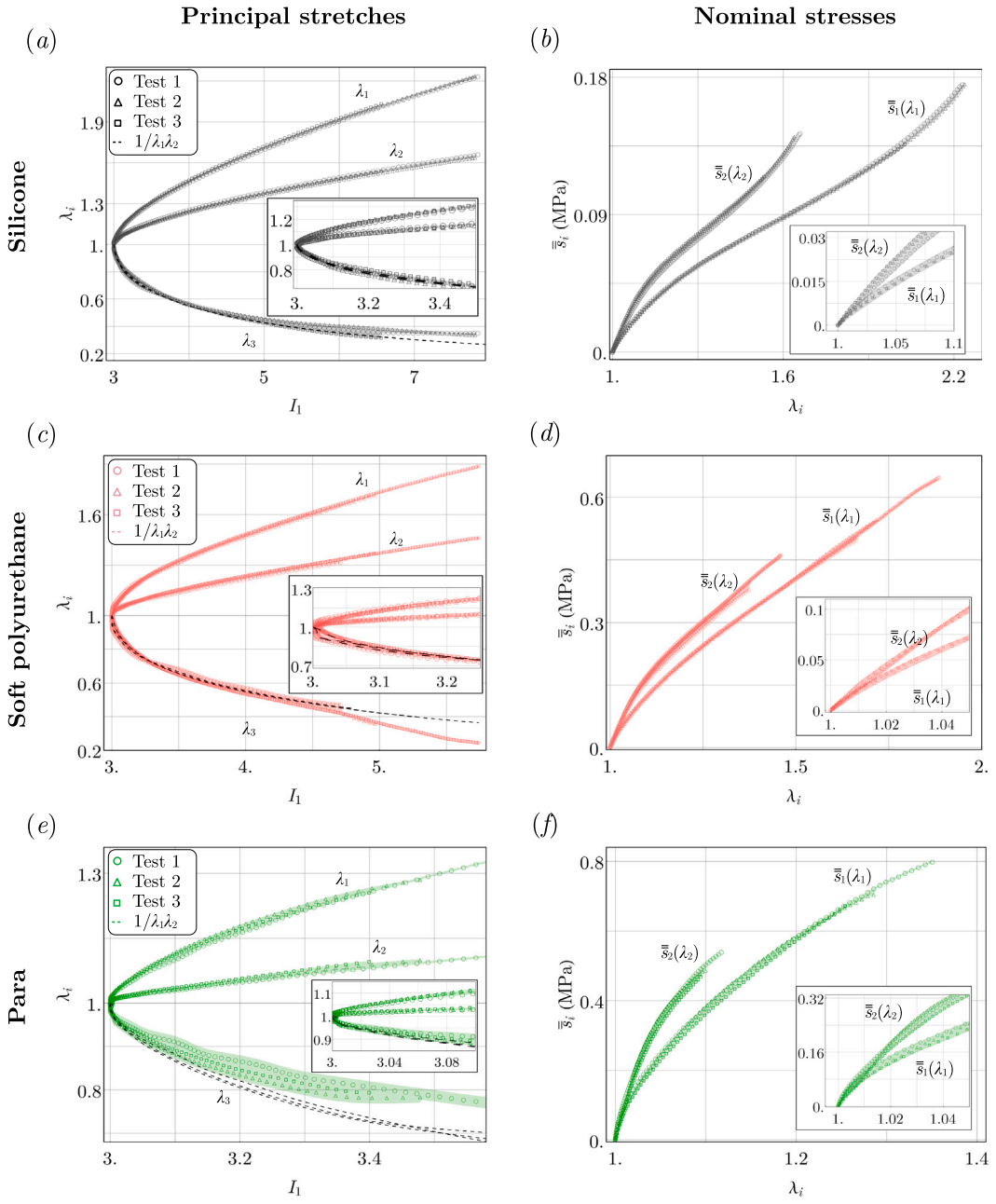

Fig. 4. Principal stretches λ_i as a function of the first deformation invariant of the Cauchy–Green deformation tensor I_1 (first column) and nominal stresses $\bar{\bar{s}}$ (second column): (a, b) silicone rubber; (c, d) soft polyurethane; (e, f) para rubber. Black dashed lines in the first column represent the behaviour of incompressible material $\lambda_3 = 1/\lambda_1\lambda_2$. Each type of marker denotes a different repetition of the test on the same rubber specimen (circular, triangular, and squared markers). The filled regions are the margins of uncertainty.

The hardening in the stress–stretch relation of the silicone in Fig. 4(b) is ascribable to the sole term W_1, which is the only one that exhibits hardening in Fig. 5(a). This is not a foregone behaviour. The uncertainties of the DEF using invariants K_i are extremely low and the associated trends, starting from 0, have a more manageable form for each of the investigated materials.

A strong interest is aroused by understanding which DEF, within the same approach, plays the more important role. In terms of invariant I_i, it is without doubt W_1 that is used in Fig. 6(b) to normalize W_2 and W_3. Except for the low value of deformations where uncertainty dominates, ratios W_i/W_1 are always less than the unit. The relative importance of terms W_2 and W_3 decreases as deformation increases but, for some materials and some ranges of deformation, they are far from negligible for low strain values. The torsion tests by Falope et al. (2024) also provide evidence of this behaviour. The energy of some hyperelastic material, such as

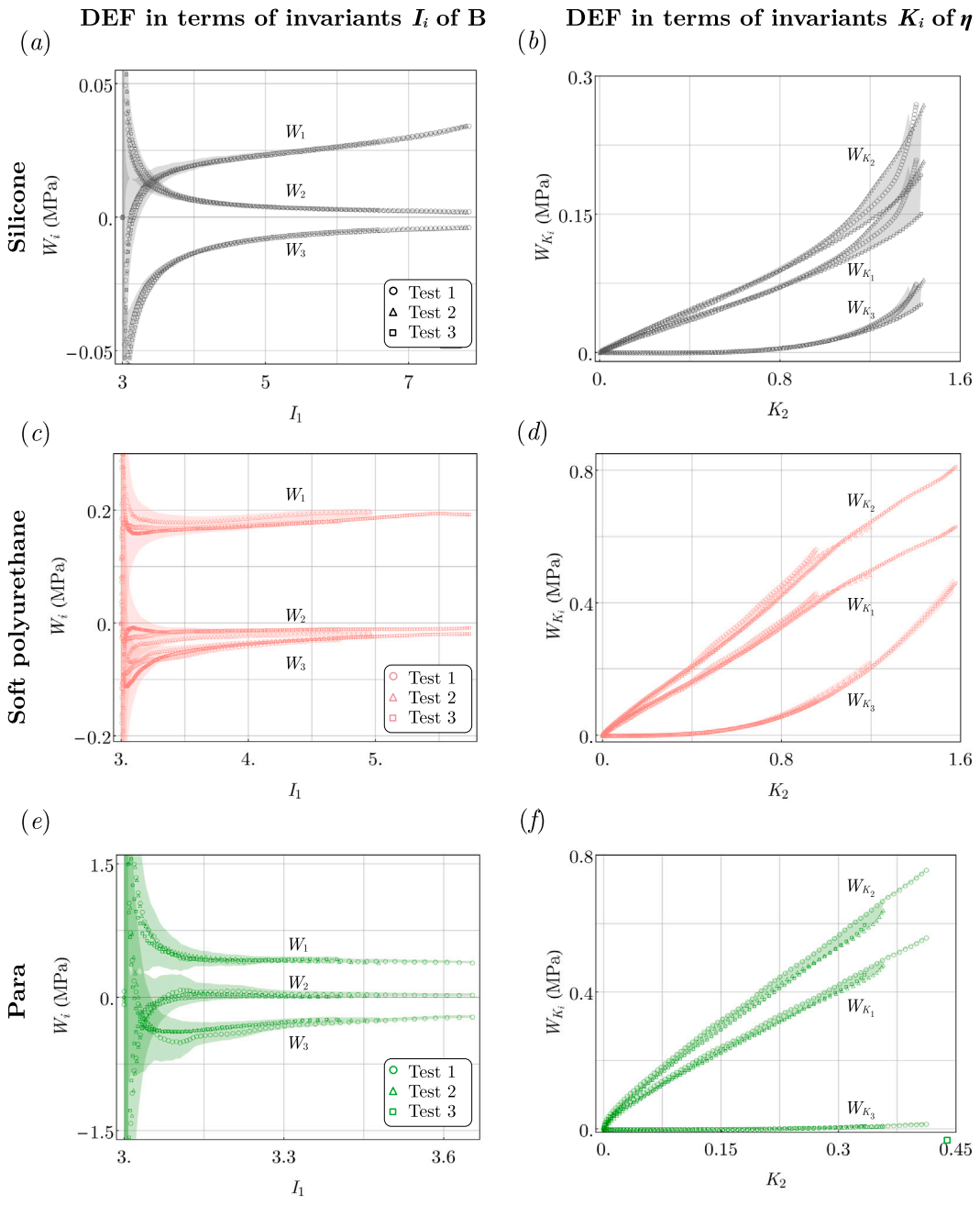

Fig. 5. Experimental values of the derivatives of the energy function, $W_i = \partial W/\partial I_i$ form (12) (first column) and $W_{K_i} = \partial W/\partial K_i$ from (16) (second column) for compressible isotropic materials: (a, b) silicone rubber; (c, d) soft polyurethane; (e, f) para rubber. Each type of marker denotes a different repetition of the test on the same rubber specimen (circular, triangular, and squared markers). The filled regions are the margins of uncertainty. For all the functions plotted, besides the variable considered, all the invariants vary.

the silicone at hand, must include the dependence of I_2 (Horgan and Smayda, 2012; Anssari-Benam et al., 2021). Far from small deformations, it is reasonable to consider the hierarchy $W_1 > W_2 > W_3$.

In the second column of Fig. 5, the DEF W_{K_i} offer a more regular trend that W_i. The full decoupling between hydrostatic and deviatoric parts of representation (13) provides a more objective and meaningful interpretation of the ratios between the DEF W_{K_i} and W_{K_2} shown in Fig. 6(c). W_{K_2}, which is the energy variation for the magnitude of distortion, is chosen as a normalization parameter because it plays the most important role. The normalized values W_{K_i}/W_{K_2} always lie below the unit. We found that the ratio W_{K_1}/W_{K_2} is not far from a nearly constant value of 0.8 . The reason for this value is due to the type of test. In the case of equi-biaxial tension ($K_3 = -1$), which is partially exhaustive for the formulation in the invariants K_i, we have $\mathbf{Y} = 0$, and the BVP

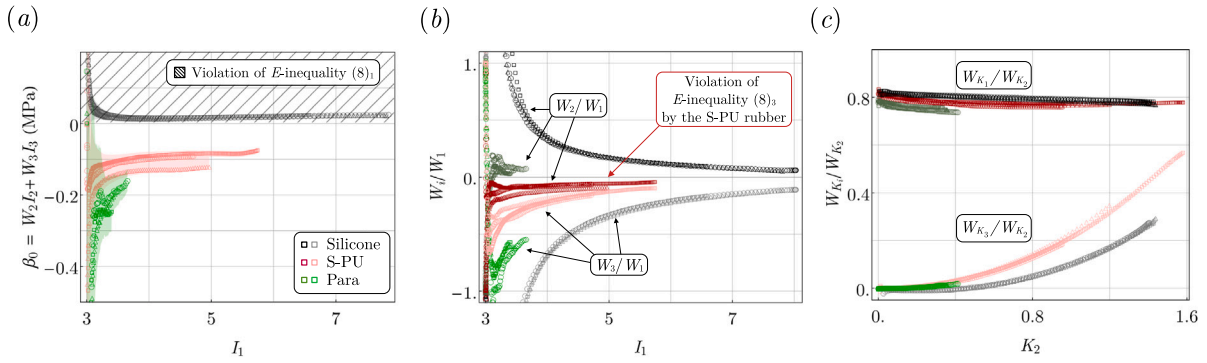

Fig. 6. Combinations of the derivatives of the energy function $W_i = \partial W/\partial I_i$ or $W_{K_i} = \partial W/\partial K_i$: (a) experimental behaviour of the empirical (E) inequality $(8)_1$ and its violation by the silicone rubber; (b) derivatives of the energy function W_i normalized for W_1 (relative weight); (c) derivatives of the energy function W_{K_i} normalized for W_{K_2}. Black, pink, and green tones denote experiments on silicone, soft polyurethane, and para rubber. Each type of marker represents a different repetition of the test on the same rubber specimen (circular, triangular, and squared markers).

problem (13) provides

$$W_{K_1} = \frac{2\lambda\bar{\bar{s}}\log\left(\frac{\lambda}{\lambda_3}\right)}{\log\left(\frac{\lambda}{\lambda_3^3}\right) - 2\log\left(\frac{1}{\lambda}\right)}, \quad W_{K_2} = \frac{\sqrt{6}\lambda\bar{\bar{s}}\log\left(\frac{\lambda}{\lambda_3}\right)}{\log\left(\frac{\lambda}{\lambda_3^3}\right) - 2\log\left(\frac{1}{\lambda}\right)}. \tag{17}$$

From (17), it is straightforward to observe that $W_{K_1}/W_{K_2} = \sqrt{2/3} \approx 0.8$. Among the material tested, during our unequal-biaxial test $-1 \le K_3 \le -0.5$. The more K_3 deviates from -1, the more the test differs from an equi-biaxial test. The weak non-linear decreasing trend of W_{K_1}/W_{K_2}, observed in Fig. 6, shows that as K_3 increases, this DEF ratio decreases slightly but may appear to approach a constant value.

A good overlapping between the measured behaviour of λ_3 and its behaviour in case of incompressibility conditions is displayed by the dashed curves in the first columns of Fig. 4. Thus, in the next Section, we investigated the experimental 2D behaviour of DEF assuming incompressible materials.

3.3. Incompressible materials: the equilibrium paths

The equilibrium path of DEF W_i can now be introduced in Fig. 7, where the projections of the equilibrium paths on the coordinated planes are also reported. The trace of all equilibrium paths on the invariant plane $I_1 - I_2$ always lies inside the *Attainable Region* of elastic materials (Currie, 2004), as the principal stretches are real. These plots are the experimental equilibrium path of each test, which lie on surfaces $W_i(I_1, I_2)$. Since different paths on the equilibrium surface describe different kinematics of the test, i.e. a different test mode, only exhaustive or partially exhaustive tests (see Corollary 2.1) can contribute to adding other paths over the equilibrium surface forming the entire surface of DEF.

For unequal-biaxial tests approached in the Cauchy–Green invariants, the only way to add and thicken the points on this graph is to execute different unequal-biaxial tests characterized by different load ratios $\bar{\bar{s}}_1/\bar{\bar{s}}_2$. In this regard, the idea of performing an iso-invariant plot of one variable (Rivlin and Saunders, 1951; Jones and Treloar, 1975; Criscione, 2004; Kulwant et al., 2023), where one of the invariants is kept fixed and the remaining represents the only variable, requires a wide experimental campaign.

The DEF in terms of Hencky invariants (14) are provided separately in Figs. 8 and 9. For W_{K_2} only, the uniaxial tests (Corollary 2.3) are partially exhaustive, and thus, they can be grouped on the same plots of the unequal-biaxial tests. In virtue of the energetic exhaustiveness, the insights on W_{K_2} are optimized and interconnected. Each test, uniaxial and unequal-biaxial, can be plotted aside in the first column of Fig. 8, enforcing and corroborating the identification of the equilibrium surface W_{K_2}. The second column of the figure contains the detail of the equilibrium path of the sole unequal-biaxial tests. The advantage of energetic exhaustiveness eliminates the usual requirement of simultaneous fitting of non-congruent quantities, producing commensurable results. The fitting procedure can be directly done on the surface of DEF. Pure shear tests ($K_3 = 0$) would increase the resolution of the equilibrium paths of Fig. 8 by allowing a highly dense interpolation of the surface W_{K_2}. However, we discuss in Section 3.4 that exhaustive tests can be specifically designed to produce highly dense data to reach an accurate description of the DEF. For unequal-biaxial and uniaxial tests, both K_2 and K_3 vary in Fig. 8, on the contrary, in the uniaxial tests (blue cross markers) K_3 is constant. Blue markers of uniaxial tests delimit the boundaries of the DEF domain. The behaviour of W_{K_3} is shown in Fig. 9. Since uniaxial tests approached in the invariants K_i are only partially exhaustive, they do not provide information on W_{K_3}. Thus, Fig. 9 reports only the results of the unequal-biaxial test. Such behaviour is far from allowing us to define the surface W_{K_3} because too sparse points are presented.

Looking at Figs. 8 and 9, one of the main observations concerns the distribution and density of the points provided by the tests over domain $K_2 \in [0, +\infty]$ and $K_3 \in [-1, +1]$. All tests have an equilibrium path that develops from $K_2 = 0$, which is the undeformed

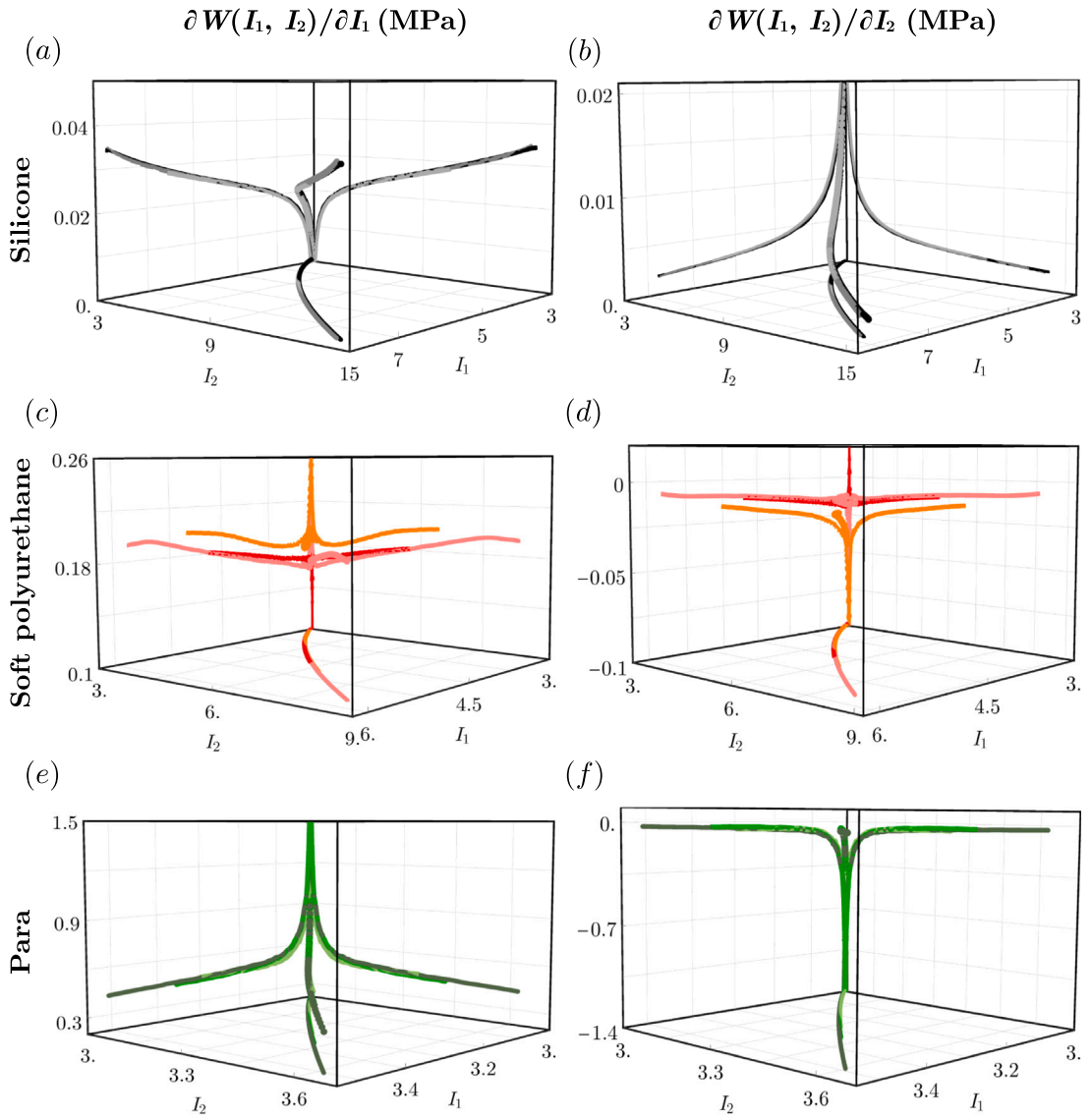

Fig. 7. Experimental values of the derivatives of the energy function $W_1 = \partial W/\partial I_1$ (first column) and $W_2 = \partial W/\partial I_2$ (second column) for incompressible isotropic material computed using (A.4): (a, b) silicone rubber Dragon Skin FX-Pro; (c, d) soft polyurethane Vytaflex 30; (e, f) para rubber. The projection onto the horizontal plane and the main planes $I_1 = 3$ and $I_2 = 3$ are provided.

configuration characterized by a null amount of distortion, towards the greatest values of K_2. Equilibrium paths of uniaxial tests develop at constant values of K_3. Tests at some constant values of K_2 should be carried out to increase knowledge of the equilibrium surface and allow for an accurate definition of the DEF $W_{K_i}(K_2, K_3)$. If well designed, can the energetic exhaustiveness of the unequal-biaxial test alone provide all the information necessary for the comprehensive determination of DEF?

3.4. Optimized insight on DEF by design of exhaustive tests

We now focus on the iso-invariant equilibrium path ($K_2 = const$ and $K_3 = const$), not for their meaning but for the information provided. Equilibrium surfaces of DEF are known as a function of variables K_i (or analogously λ_i). Thus, it is of particular interest to analyse the traces of some characteristic equilibrium paths on the $K_2 - K_3$ plane, which identifies the type of the test.

The iso-invariant equilibrium paths at a constant value of K_3 depict the uniaxial tension/equi-biaxial compression, uniaxial compression/equi-biaxial compression, and the pure shear test, respectively for K_3 =+1, −1, and 0. These are distinct paths

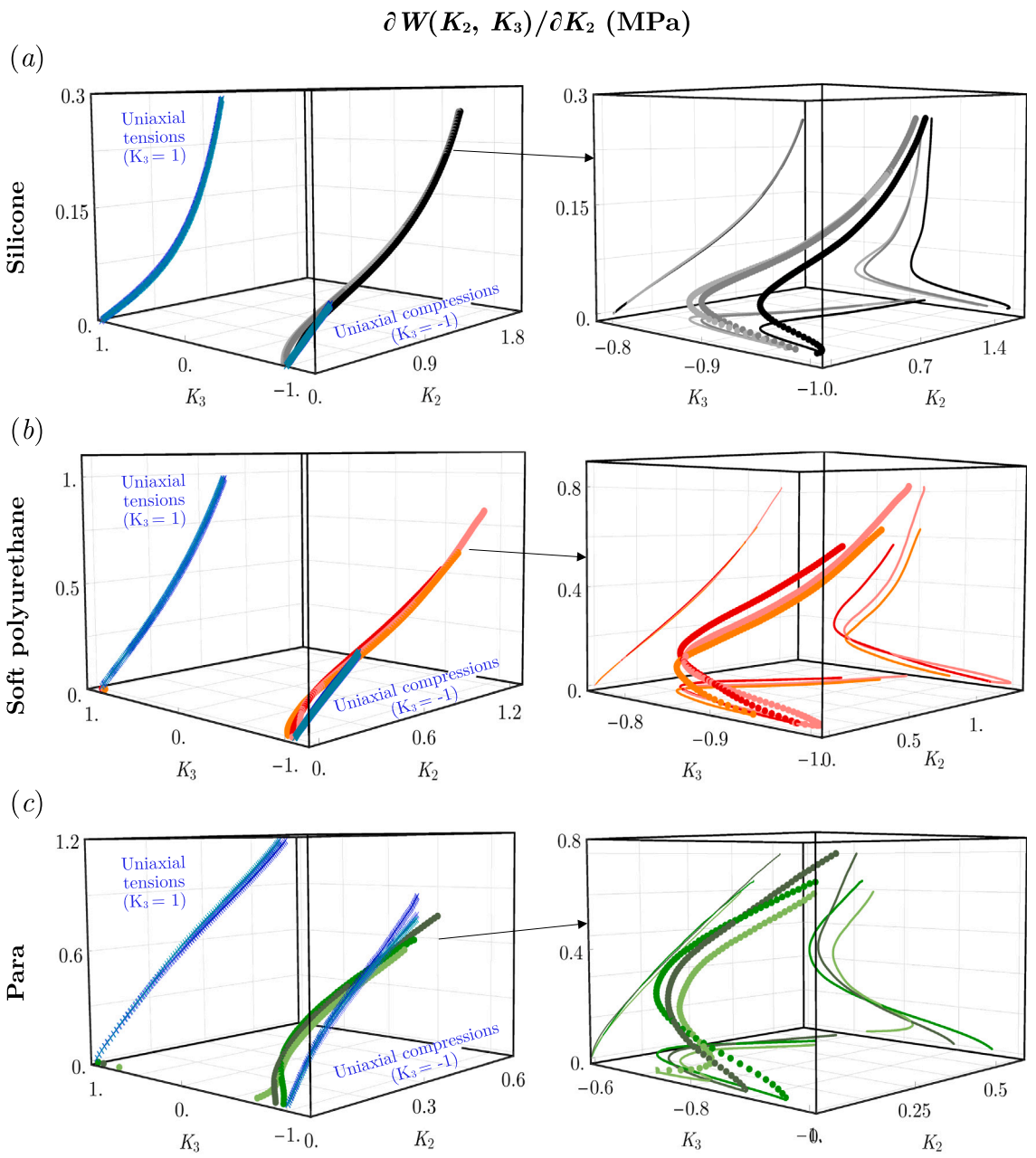

Fig. 8. Experimental values of the derivative of the energy function $W_{K_2} = \partial W/\partial K_2$ in case of incompressible material computed using $(A.6)_1$: (first column) unequal-biaxial and uniaxial test plotted in the same domain, as the tests are energetically exhaustive for W_{K_2}; (second column) detail of the unequal-biaxial test only. (a) silicone rubber Dragon Skin FX-Pro; (b) soft polyurethane Vytaflex 30; (c) para rubber. Blue markers denote uniaxial tension ($K_3 = +1$) and uniaxial compression ($K_3 = -1$).

associated with different modes of distortion. However, from $(14)_3$, one has that also $\lambda_2 = 1$ gives $K_3 = 0$ in case of incompressible materials. The pure shear of incompressible materials corresponds to a constrained unequal-biaxial. The traces of some particular equilibrium paths are plotted in Fig. 10(a).

The traces of uniaxial tests delimit the upper and lower boundaries of the domain of the DEF, $K_3 \in [-1, 1]$. However, an accurate recovery of the 2D behaviour of the DEF requires extensive knowledge of additional equilibrium paths within the K_3 domain shown in Fig. 10(a). The introduction of the strain ratio parameter α, which is the ratio between the principal engineering strains, $\alpha = \varepsilon_2/\varepsilon_1$, shows the wide range of (horizontal) equilibrium paths recovered by the unequal-biaxial tests.

We are now looking for a simple relation between the principal stretches that guarantees the equilibrium path at constant K_2. These paths enforce and corroborate the identification of the equilibrium surfaces of DEF, W_{K_2} and W_{K_3}, since they develop in the

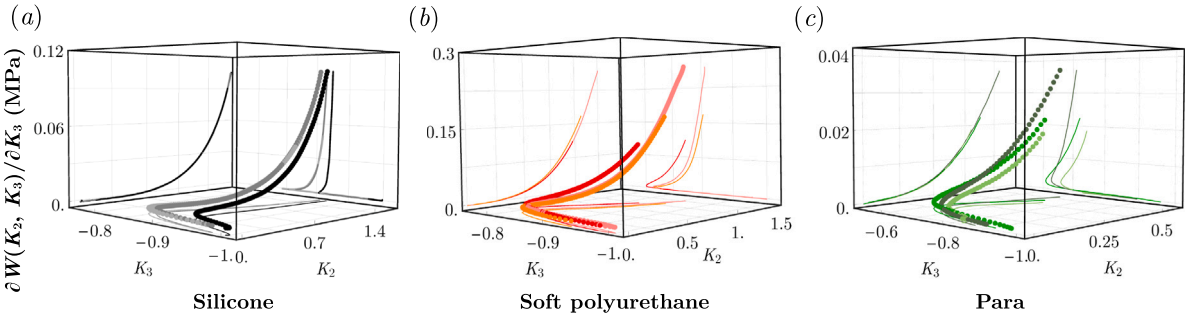

Fig. 9. Experimental values of the derivative of the energy function $W_{K_3} = \partial W/\partial K_3$ in case of incompressible material computed using $(A.6)_2$: (a) silicone rubber; (b) soft polyurethane; (c) para rubber. The results of uniaxial tests cannot be included, as they are partially exhaustive and non-exhaustive for W_{K_3}.

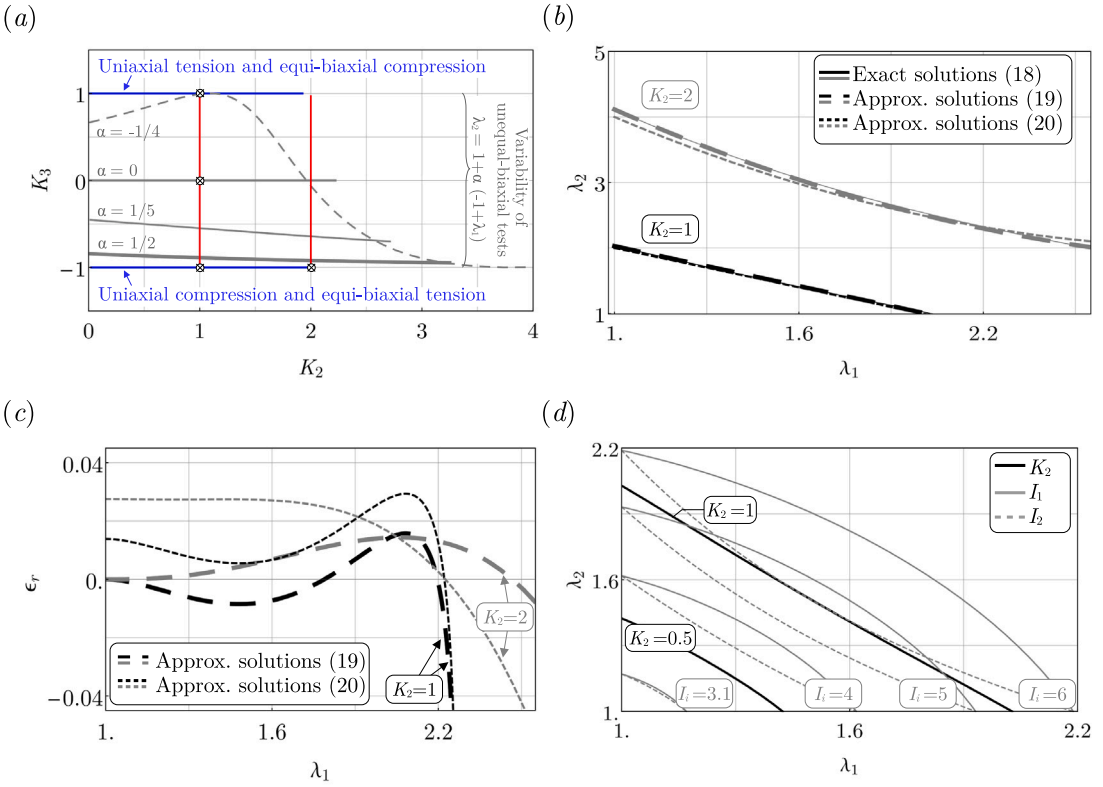

Fig. 10. Kinematic relations: (a) traces on the invariant plane $K_2 - K_3$ showing some characteristic equilibrium paths of uniaxial and equi-biaxial tests (blue lines), unequal-biaxial tests varying the engineering strain ratio $\alpha = \varepsilon_2/\varepsilon_1$ (grey curves), and iso-K_2 paths (red lines); (b) exact and approximated relations between principal stretches providing the iso-K_2 paths for unequal-biaxial test; (c) relative errors between the exact and approximated relations of iso-K_2 paths; (d) comparison between iso-invariant paths formulated in terms of the invariants of the Cauchy–Green deformation tensor (I_1 and I_2) and the Hencky strain tensor (K_2).

vertical direction (see red curve of Fig. 10(a)) connecting different standard tests. For unequal-biaxial tension with K_2 constant, from relation (14) one has

$$\lambda_2(\lambda_1, K_2) = e^{\frac{1}{2}\left(\sqrt{2K_2^2 - 3\log^2\lambda_1} - \log\lambda_1\right)}. \tag{18}$$

We consider $K_2 = 2$ a large amount of distortion and so Eq. (18) is plotted in Fig. 10(b) for $K_2 = 1$ and 2. This relationship can be significantly simplified, providing a compact formula for designing an iso-K_2 test. By considering some integer values of K_2, we

obtain the following compact relations:

$$\begin{aligned} &\text{for } K_2 = 1, \quad \lambda_2 = e^{\frac{1}{\sqrt{2}}}\left[1 - \frac{1}{2}\left(\lambda_1 - 1\right)\right] + O\left((\lambda_1 - 1)^2\right), \\ &\text{for } K_2 = 2, \quad \lambda_2 = e^{\sqrt{2}}\left[1 - \frac{1}{2}\left(\lambda_1 - 1\right) + \frac{3}{16}\left(2 - \sqrt{2}\right)\left(\lambda_1 - 1\right)^2\right] + O\left((\lambda_1 - 1)^3\right). \end{aligned} \tag{19}$$

These two relations stem from the series expansion around the reference configuration, up to the order $n = K_2$. The approximations (19) are shown in Fig. 10(b) over a physically reasonable range of deformation. These ensure a relative error lower than 2%, as depicted in Fig. 10(c). A second approximation facilitates a straightforward understanding of the relationships (19). Rounding the coefficients of $(\lambda_1 - 1)$ in Eq. (19) to 1/2 yields

$$\begin{aligned} &\text{for } K_2 = 1, \quad \lambda_2 \approx 3 - \lambda_1, \\ &\text{for } K_2 = 2, \quad \lambda_2 \approx 4 - 2(\lambda_1 - 1) + \frac{1}{2}(\lambda_1 - 1)^2. \end{aligned} \tag{20}$$

The dotted curves of Fig. 10(b) and (c) show the results of Eq. (20) and the associated relative errors. Iso-K_2 tests can be performed by prescribing a rational displacement rate, starting from a pre-stretched condition, followed by a relaxation-controlled test along direction 2, and tension in direction 1.

Along the iso-invariant path $K_2 = 1$, the principal invariants I_1 and I_2 range from 4.7 to 5.5. Fig. 10(d) shows the iso-invariant path on the space of principal stretches in terms of $K_2 = 0.5$ and 1, and $I_i = 3.1, 4, 5, 6$. As these values increase, the invariants I_i exhibit a more pronounced non-linearity than K_2. This is inherent in the definition of such invariants. This additionally sheds light on the most marked feasibility of unequal-biaxial characterization using the Lode invariants than the principal invariants I_i.

4. Concluding remarks

In this study, we have defined *energetically exhaustive* tests, presented two alternative forms of Baker–Ericksen constitutive inequalities, demonstrated the violation of two empirical inequalities, and discussed the homothetic tests required for a 2D comprehensive representation of the derivative of the energy function (DEF). Neither all states of deformation nor all deformation measures provide direct information on each DEF. These findings have been reinforced by experimental evidence of unequal-biaxial tests on three rubbers.

A test has been defined as energetically exhaustive (Definition 2.1) if its matrix form associated with its elastic boundary value problem is equivalent to a determined system of equations in the unknowns DEF. This definition, along with the definitions of non-exhaustive and partially exhaustive tests, has led to two relevant corollaries of the Rouché–Capelli theorem. These corollaries are of crucial importance. The choice of a deformation measure, be the Cauchy deformation tensor or the Hencky strain tensor, can yield the same test to be energetically partially-exhaustive or non-exhaustive (Corollary 2.1–Corollary 2.4, Propositions 2.1, and 2.2).

Baker and Ericksen (1954) and empirical inequalities have been recalled and two alternative forms of *BE*-inequalities have been presented. It has been demonstrated that the *BE*-inequalities and their alternative forms represent the balance conditions of non-exhaustive tests.

Experiments on unequal-biaxial tests of three different rubbers have been presented, along with the uncertainty analysis allowed by the repetition of the tests. The results have confirmed that the uncertainty associated with the DEF of Cauchy–Green deformation tensors leads to relevant uncertainties and singular behaviour for small deformations. In contrast, using invariants of Hencky strain tensor regularizes the behaviour of the DEF and reduces the associated experimental uncertainty.

Among the three materials tested, experiments have contradicted empirical inequality $\beta_0 \leq 0$ and $\beta_{-1} \leq 0$ bringing to light the empirical and hierarchical inequalities $W_1 > W_2 > W_3$. Being empirical in nature, violation of the *E*-inequalities does not invalidate the experiments. On the contrary, the experiments appear to invalidate or question the need for the *E*-inequalities. Therefore, the *E*-inequalities may not be appropriate for some materials. In terms of DEF W_{K_i}, we found that W_{K_3}, which is associated with the mode of distortion, is always less than the other terms and the ratio W_{K_1}/W_{K_2} has nearly constant values equal to 0.8.

The experiments have supported the nearly incompressible condition of the rubber. Under this reasonable assumption, the equilibrium paths lying on the surfaces $W_{K_2}(K_2, K_3)$ and $W_{K_3}(K_2, K_3)$ have been provided. However, in our opinion, the obtained equilibrium paths and the data available in the literature are not sufficiently dense to interpolate data and recover the surface of the DEF. This is because the equilibrium paths from the standard tests provide too sparse data. Thus, we have shown that, if well-designed and using the proposed accurate and approximated formula (20), the unequal-biaxial tests alone are sufficient to thicken experimental data to comprehensively describe the surface of the DEF, i.e. the response function of the materials.

CRediT authorship contribution statement

Federico Oyedeji Falope: Writing – review & editing, Writing – original draft, Visualization, Validation, Methodology, Investigation, Formal analysis, Data curation, Conceptualization. **Luca Lanzoni:** Writing – review & editing, Funding acquisition. **Angelo Marcello Tarantino:** Writing – review & editing, Funding acquisition.

Declaration of competing interest

The authors declare that they have no known competing financial interests or personal relationships that could have appeared to influence the work reported in this paper.

Data availability

Data will be made available on request.

Acknowledgements

F.O.F gratefully acknowledges the support of the National Group of Mathematical Physics (GNFM-INdAM). L.L. gratefully acknowledges financial support from the Italian Ministry of Research (MUR) through the research grant PRIN 2022 PNRR "New challenges of thin-walled structures at large strains and their promising applications" (prot. P2022AHFCP; CUP C53D23008220001) and financial support from University of Modena and Reggio Emilia in the framework of the project "FAR Dipartimentale 2023-2024" (CUP:E93C23000280005). A.M.T gratefully acknowledges the financial support of the MUR through the research grant PRIN 2022 PNRR "Energy harvesting via naturally induced piezoelectric vibration with a view towards application" (prot. P2022ATTAR; CUP B53D23026940001).

Appendix A. Derivatives of the energy functions for incompressible materials

For isotropic and incompressible materials ($\det \mathbf{F} = 1$), the Cauchy stress tensor

$$\mathbf{T} = -p\mathbf{I} + 2W_1\mathbf{B} - 2W_2\mathbf{B}^{-1} \tag{A.1}$$

includes the unknown Lagrange multiplayer p which introduces the incompressibility condition, i.e. the internal pressure. Analogously to system (10), the cases of homothetic deformations lead to the following explicit form of the BVP:

$$\begin{cases} -p\lambda_1^{-1} + 2\left(W_1\lambda_1 - W_2\lambda_1^{-3}\right) = \bar{\bar{s}}_1 \\ -p\lambda_2^{-1} + 2\left(W_1\lambda_2 - W_2\lambda_2^{-3}\right) = \bar{\bar{s}}_2 \\ -p\lambda_1\lambda_2 + 2\left(W_1\lambda_1^{-1}\lambda_2^{-1} - W_2\lambda_1^{3}\lambda_2^{3}\right) = \bar{\bar{s}}_3 \end{cases}. \tag{A.2}$$

For unequal-biaxial tests ($\bar{\bar{s}}_i = \bar{s}_i$ and $\bar{s}_3 = 0$), the equilibrium $(A.2)_3$ provides the hydrostatic pressure as

$$p = 2\left(\frac{W_1}{\lambda_1^2\lambda_2^2} - \lambda_1^2\lambda_2^2 W_2\right). \tag{A.3}$$

By introducing the hydrostatic pressure (A.3) into (A.2), the DEF become (Rivlin and Saunders, 1951)

$$\begin{cases} W_1 = \lambda_1^2\lambda_2^2\,\dfrac{\left(\lambda_1^2\lambda_2^4 - 1\right)\lambda_1^3\bar{s}_1 + \left(1 - \lambda_1^4\lambda_2^2\right)\lambda_2^3\bar{s}_2}{2\left(\lambda_1^2 - \lambda_2^2\right)\left(\lambda_1^4\lambda_2^2 - 1\right)\left(\lambda_1^2\lambda_2^4 - 1\right)} \\ W_2 = \lambda_1^2\lambda_2^2\,\dfrac{\left(1 - \lambda_1^2\lambda_2^4\right)\lambda_1\bar{s}_1 + \left(\lambda_1^4\lambda_2^2 - 1\right)\lambda_2\bar{s}_2}{2\left(\lambda_1^2 - \lambda_2^2\right)\left(\lambda_1^4\lambda_2^2 - 1\right)\left(\lambda_1^2\lambda_2^4 - 1\right)} \end{cases}. \tag{A.4}$$

In terms of Hencky strain tensor $\boldsymbol{\eta}$ and its invariants K_i (14), incompressibility condition implies $K_1 = 0$ and $W = W(K_2, K_3)$. Thus, Cauchy stress (13) has an isochoric component associated with the Lagrange multiplier and a deviatoric component associated with $\boldsymbol{\eta} = \boldsymbol{\eta}^d$, namely

$$\mathbf{T} = -p\mathbf{I} + W_{K_2}\boldsymbol{\Phi} + \frac{W_{K_3}}{K_2}\mathbf{Y}. \tag{A.5}$$

Using (A.5), the BVP of the unequal-biaxial tests provides the Lagrange multiplier as

$$p = \frac{1}{K_2^2}\log\left(\frac{1}{\lambda_1\lambda_2}\right)\left[3K_3W_{K_3} - K_2W_{K_2} - 3\sqrt{6}\log\left(\frac{1}{\lambda_1\lambda_2}\right)\frac{W_{K_3}}{K_2}\right] + \frac{\sqrt{6}W_{K_3}}{K_2}$$

which, introduced into (A.5), gives the DEF as

$$\begin{cases} W_{K_2} = \dfrac{\lambda_1\bar{s}_1\log\left(\lambda_1\right) + \lambda_2\bar{s}_2\log\left(\lambda_2\right)}{K_2} \\ W_{K_3} = \dfrac{K_2^3\left[\lambda_1\bar{s}_1\log\left(\lambda_1\lambda_2^2\right) - \lambda_2\bar{s}_2\log\left(\lambda_1^2\lambda_2\right)\right]}{3\sqrt{6}\log\left(\frac{\lambda_1}{\lambda_2}\right)\log\left(\lambda_1^2\lambda_2\right)\log\left(\lambda_1\lambda_2^2\right)} \end{cases}. \tag{A.6}$$

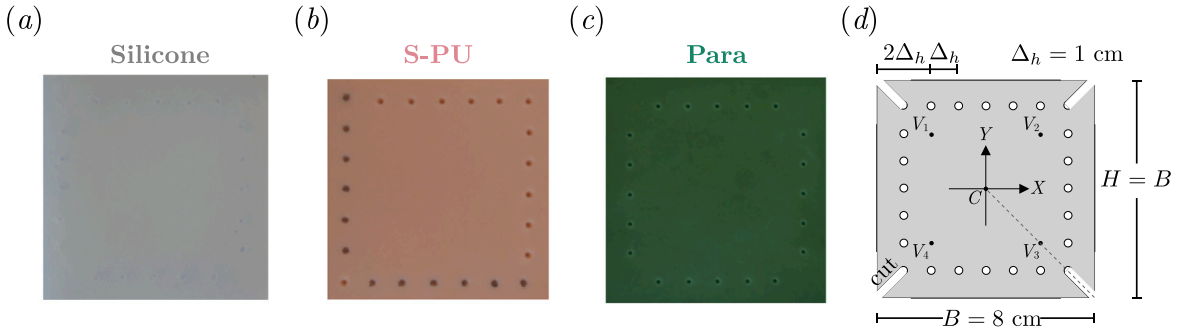

Fig. B.11. Rubber specimens used in the unequal-biaxial test: (a) silicone rubber Dragon Skin FX-Pro; (b) soft polyurethane Vytaflex 30; (c) para rubber; (d) geometries of the samples, hole for hook anchoring, and cuts to promote homogeneous deformations.

Table B.2
Thickness of the rubber samples (mm) measured at the four vertices V_i (10 mm inside the cuts on the diagonals) and the centre of the specimen, including mean values and standard deviation. The mean values are used to compute nominal stress and transversal stretch λ_3.

Rubber	V_1	V_2	V_3	V_4	C	Mean ± St.dev
Silicone	9.343	9.603	9.503	9.543	9.443	9.487 ± 0.099
S-PU	4.696	4.599	4.498	4.471	4.489	4.550 ± 0.095
Para	2.922	2.952	2.952	2.892	3.052	2.954 ± 0.060

Appendix B. Experiments

B.1. The materials

Three rubber-like materials are tested: a soft polyurethane rubber (VytaFlex 30, https://www.smooth-on.com/products/vytaflex-30/) with a hardness value of 30 ShA, associated with pink tones, and denoted with S-PU (soft polyurethane); a silicone rubber (Dragon Skin FX-Pro, https://www.smooth-on.com/products/dragon-skin-fx-pro/) with a hardness value of 2 ShA and associated with grey tones; and a para rubber (https://www.fimospa.it/prodotto/elastomeri-compatti/) with a hardness value of 45 ShA and associated with green tones. Uniaxial tests (tension and compression merged) are also carried out following the procedure detailed in Falope et al. (2024) and reported in Appendix C. For the same specimen and each type of rubber, unequal-biaxial experiments were repeated three times to assess the repeatability of tests.

The geometries of the specimens used for unequal-biaxial tests are reported in Fig. B.11. The specimens have a square shape of 80 mm. Along each side of the samples seven equispaced holes, with interspace of 10 mm, are realized for the anchoring system with hooks. Cuts were made at the perimeter holes to promote homogeneous deformations. Specimen thickness is measured on 5 points of the specimen, at the centroid and on the principal diagonals at 15 mm from the final holes (see Table B.2). The thickness of the specimen was measured using optical laser instrumentation described in the following. The average thickness is used to evaluate the through-the-thickness (transversal) stretch λ_3 and nominal stress. The width of the specimen used for nominal stress is 60 mm.

Geometries of the samples were taken after the conditioning phase. The conditioning phase consisted of a pre-stress corresponding to half of the maximum load reached along direction 1 (since many tests were carried out before the main tests). The temperature was not controlled and ranged between 19 and 25 °C (room temperature). After conditioning, which was maintained for 5 min, stress was removed and, after another 5 min, the proper tests began. Tests ended before the failure of the specimen, which started from the clamping system (tearing of the holes).

B.2. Experimental device and monitoring

The unequal-biaxial tests were carried out with the device shown in Fig. B.12. It is composed of a steel frame organized into two levels. Level one lies on the top part of the device, while level two is placed below (see Fig. B.12(a) and (b)). At level one, the test plan includes the rubber specimen, the optical monitoring system (DIC, digital image correlation), and the punctual laser optical (PLO) device at its centre. At level two, there is the actuator and the cords-pulleys systems for load application.

At the centre of level one, the square rubber specimen is anchored with a system of hooks, which are tied to cords fixed to an aluminium triangle (Fig. B.12(a), (c), and (d)). Two load cells are positioned at the vertices of two metal triangles, one in the X direction and the other in the Y direction. Load cells measure up to 200 N with a measurement uncertainty $\Delta_{\text{cell}} = \pm 0.5$ N. At the apex of each triangle or load cell, a cord is tied as in Fig. B.12(c). From metal triangles or cells, the cord system connects to the actuator via four blocks of pulleys positioned in four different planes.

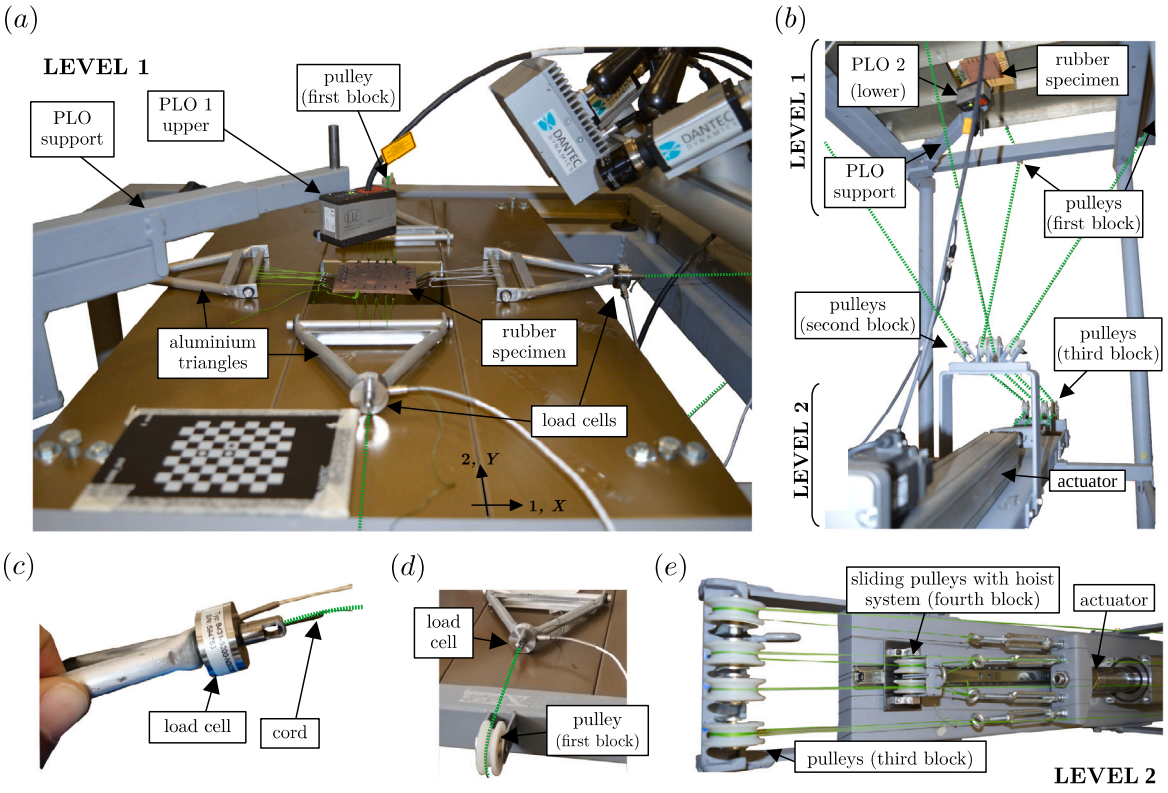

Fig. B.12. Device for unequal-biaxial test: (a) level 1 (upper part) with the rubber specimen at the centre, anchored with hooks and cord system to the aluminium triangles, punctual laser optical (PLO), load cells placed at the vertices of the triangles, and cord system that passes around the pulleys of the first block (four pulleys on each side) reached the actuator located at the level 2 (lower level); (b) lower view of the device, highlighting the cord systems and blocks of pulleys connecting the specimen with the actuator; (c) detail of the load cell; (d) sketch of the first block of pulleys; (e) detail of the level 2, including the third and fourth block of the pulley to replicate the hoist system.

The first block of pulleys is composed of four separate pulleys placed at each side of level one (Fig. B.12(a), (b), and (d)). The second block of pulleys is situated above the actuator, between level one and level two (Fig. B.12(b)). The third block of pulleys is mounted at level two in front of the actuator (Fig. B.12(b) and (e)). The fourth block, between block three and the actuator, can slide along a guide parallel to the actuator. This sliding pulley works like a hoist system, by which twice the force is transmitted to the cords associated with X direction of the specimen. In this way, the device applies a force F along the Y direction and $2F$ along the X direction. The actuator works at 100 mm/min.

The transverse stretch of the specimen, that is the out-of-plane component, is monitored using two punctual laser optical (PLO) devices. The PLO has a starting measuring range of 25 mm with an acquisition window of 25 mm and uncertainty of $\Delta_{\text{PLO}} = \pm 5\,\mu\text{m}$. The first PLO is placed above the specimen, as reported in Fig. B.12(a) and B.13(a), while the second is placed below the specimen. The arms of the PLO support allow for adjusting the position and orientation of laser beams in the centre of the specimen (centring and collimation). The difference between the distances acquired by the PLO devices provides the variation in specimen thickness (λ_3).

The optical monitoring of the in-plane displacement and stretches (λ_1 and λ_2) is carried out using two DIC cameras in a stereo mode set-up (Fig. B.12(a)). The calibration of DIC cameras provides an uncertainty of the displacement measurement $\Delta_{\text{DIC}} = \pm 10\,\mu\text{m}$. Two pairs of virtual gauges were used, represented by the points $P_1 - P_2$ and $P_3 - P_4$ of Figs. B.13(d) and (e), on the sides of the reflection region. The not acquired region, which corresponds to the centre of the specimen where a cross marker is painted, is assumed as a reference point for the principal stretches computation. Close to this region, DIC provides homogeneous deformations highlighted by the principal directions reported in Figs. B.13(d) and (e).

Appendix C. Uniaxial tests

The nominal stress vs. longitudinal stretch curve of the uniaxial test is shown in Fig. C.14(a). For each rubber of Appendix B.1, three specimens are tested under compression and three under tension. Details on the specimen geometries and test procedure are reported in Falope et al. (2024). During the test, the transversal stretch has been monitored with the DIC device. Using the logarithmic scale, the experimental relation between longitudinal stretch λ_3 and the transversal stretch λ is sketched in Fig. C.14(b)

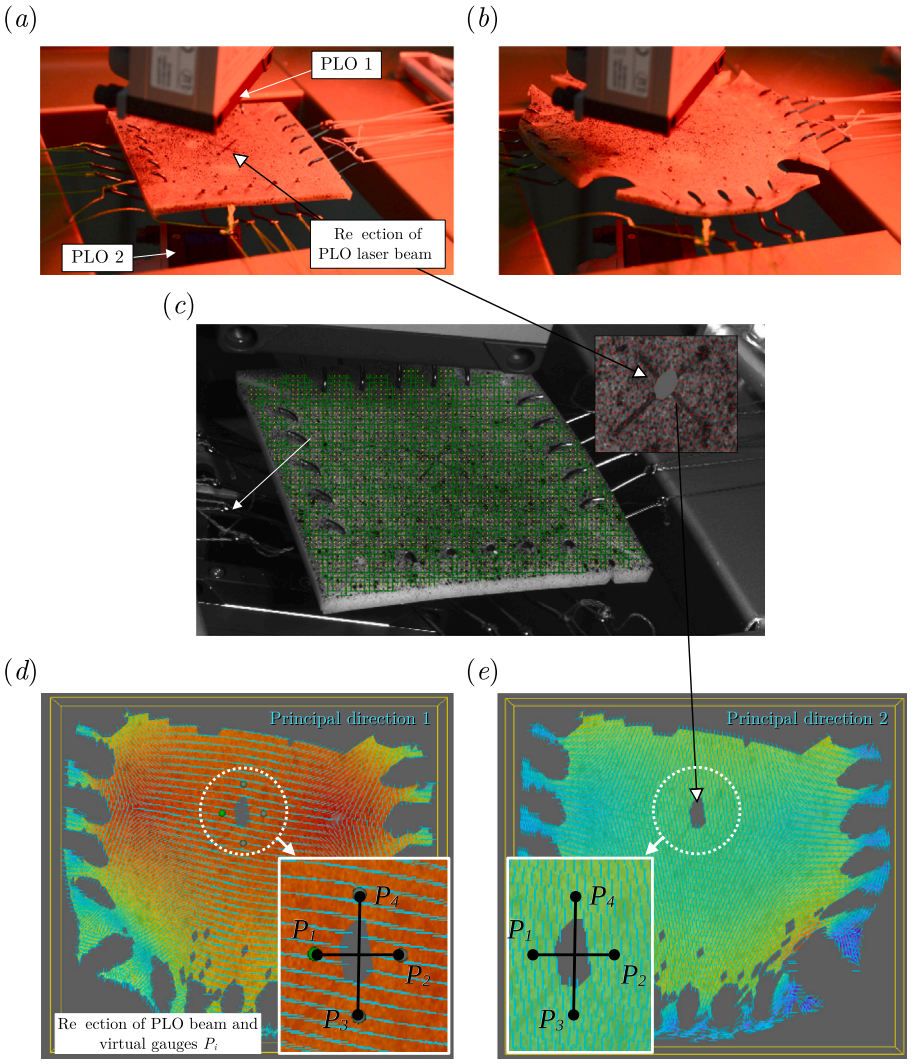

Fig. B.13. Optical acquisition of the unequal-biaxial test: (a) reference configuration of the specimen with the set-up of the punctual laser optical (PLO) devices for measuring the out-of-plane stretch; (b) deformed configuration; (c) DIC grid subdivision of the monitored surface for the measurement of the in-plane stretches, and optical interference of the DIC acquisition caused by the laser beam reflection of the PLO; (d, e) principal directions of the deformation acquired by the DIC cameras and virtual gauges $P_1 - P_2$ and $P_3 - P_4$ used to compute the in-plane stretches. Around the centre of the specimen affected by the laser reflection, the (orthogonal) principal directions oriented in the load directions highlight and support the assumption of homogeneous deformations, as they are independent of the spatial coordinate in this region.

along with the incompressibility relation $\lambda = \lambda_3^{-1/2}$. The slope of the plot $\log(\lambda_3)$ vs. $\log(\lambda^{-1})$ corresponds to the nonlinear Poisson function of the material (Beatty and Stalnaker, 1986).

The silicone and the soft polyurethane are close to being incompressible since their kinematic relation of Fig. 4(b) nearly overlaps with the incompressibility curve. This is no longer true for the natural para rubber, even at low deformations. Consistently, the same behaviour is observed during the unequal-biaxial tests (see the first column of Fig. 4).

A remarkable consistency between the results of the uniaxial test and the unequal-biaxial tests is observed. This is based on the incompressibility condition previously mentioned and the linearized elastic moduli of isotropic materials. For isotropic materials, the linearized moduli, namely the Young modulus E, shear modulus μ, and Poisson ratio ν, are linked by the relationship $\mu = E/2(1+\nu)$. Since at least for small deformation materials are incompressible, we consider $\nu = 1/2$, and so $\mu = E/3$. The linearized shear modulus can be extracted by unequal-biaxial test as $\mu = 2(W_1 + W_2)$ (Rivlin and Ericksen, 1955). Thus, using (12), Figs. C.15(a)–(c) show the behaviour of the experimental shear modulus of the three rubbers obtained by the unequal-biaxial tests. Disregarding the singular behaviour of DEF discussed in Section 3.2, we found $\mu_{\text{Sil}} = [0.048, 0.06]$, $\mu_{\text{S-PU}} = [0.028, 0.036]$, and $\mu_{\text{Para}} = [1.2, 1.8]$ MPa. Such values can be checked on the uniaxial test also. Looking at the Young modulus as $E = \partial\bar{s}/\partial\lambda_3$, shown in Fig. C.15(d), we have $E_{\text{Sil}} \in [0.09, 0.3]$, $E_{\text{S-PU}} \in [1.21, 1.62]$, $E_{\text{Para}} \in [4.15, 5.48]$, which fall in the reasonable range of $E = 3\mu$. Despite their different nature, consistency between the uniaxial test and the unequal-biaxial tests legitimates us to plot aside in Fig. 8 these tests.

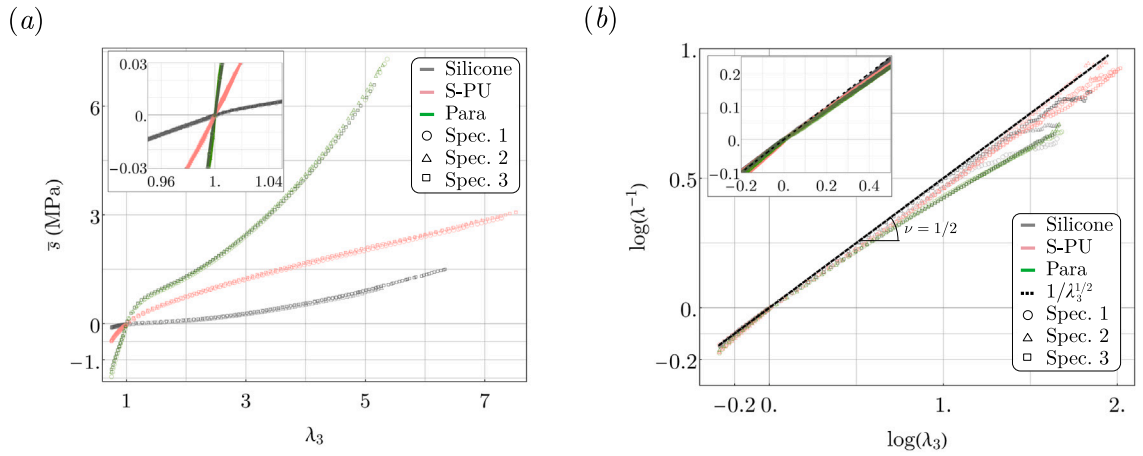

Fig. C.14. Results of the uniaxial test, compression and tension merged, of silicone rubber (grey tones), soft polyurethane rubber S-PU (pink tones), and para rubber (green tones): (a) nominal stress vs. longitudinal stretch curve; (b) logarithmic plot of transversal stretch vs. longitudinal stretch curve. The slope of the curves represents the nonlinear Poisson function (Beatty and Stalnaker, 1986) and the black dashed line represents the incompressibility curve $\lambda = \lambda_3^{-1/2}$ ($\nu = 1/2$).

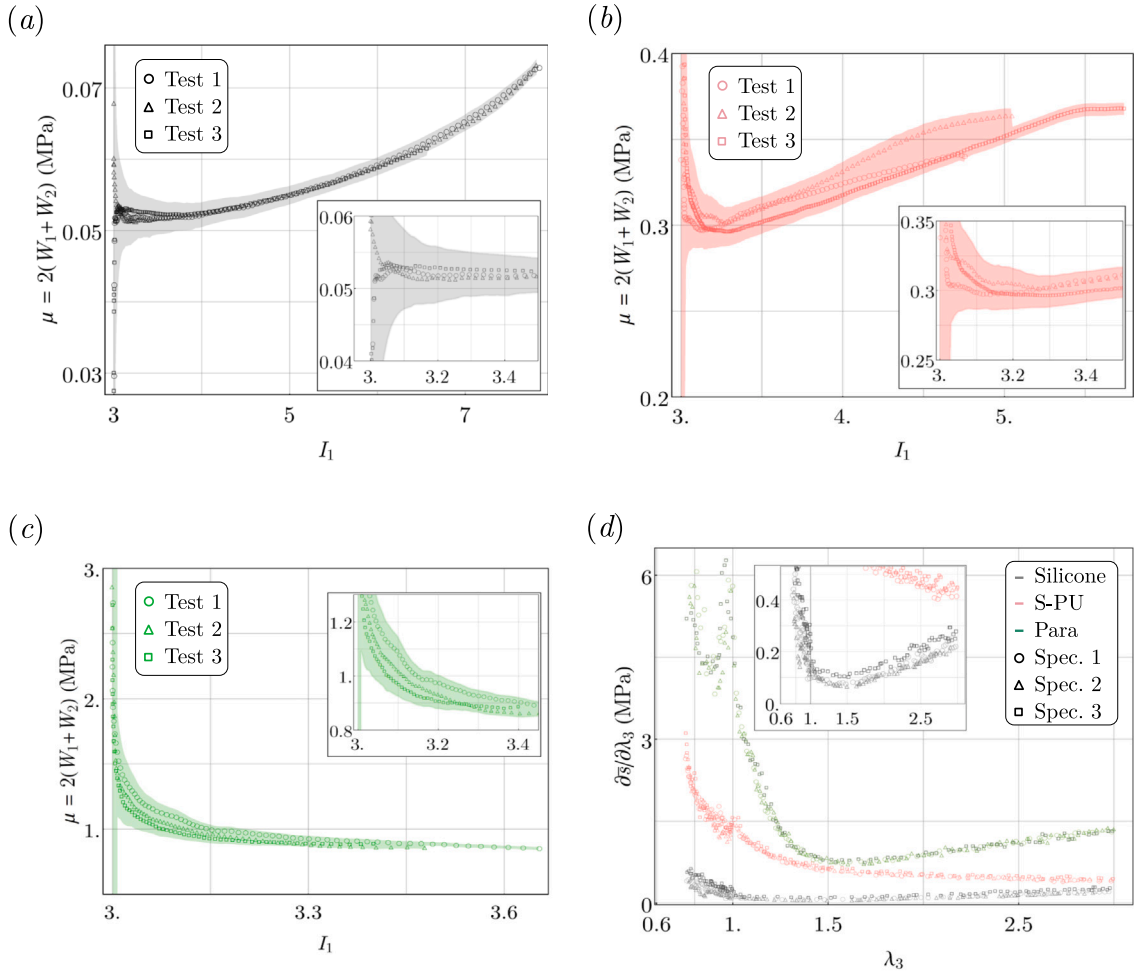

Fig. C.15. Experimental linearized elastic moduli of the rubbers under the assumption of isotropic material: (a, b, c) linearized shear modulus $\mu = 2(W_1 + W_2)$ of the silicone, soft polyurethane, and para rubber respectively, measured during unequal-biaxial tests; (d) linearized elastic modulus (Young modulus) of the materials computed as tangent modulus of the uniaxial curve ($E = \partial\bar{s}/\partial\lambda_3$). Using the incompressibility condition, the linearized Poisson ratio is $\nu = 1/2$ and so $E = 3\mu$.

References

Anssari-Benam, A., Bucchi, A., Destrade, M., Saccomandi, G., 2022. The generalised mooney space for modelling the response of rubber-like materials. J. Elasticity 151 (1), 127–141. http://dx.doi.org/10.1007/s10659-022-09889-1.

Anssari-Benam, A., Bucchi, A., Saccomandi, G., 2021. On the central role of the invariant I_2 in nonlinear elasticity. Internat. J. Engrg. Sci. 163, 103486. http://dx.doi.org/10.1016/j.ijengsci.2021.103486.

Anssari-Benam, A., Horgan, C.O., 2022. A three-parameter structurally motivated robust constitutive model for isotropic incompressible unfilled and filled rubber-like materials. Eur. J. Mech. A Solids 95, 104605. http://dx.doi.org/10.1016/j.euromechsol.2022.104605.

Ariano, R., 1925. Deformazioni finite di sistemi continui, Memoria 2. Ann. Mat. Pura Appl. 2 (1), 217–261. http://dx.doi.org/10.1007/BF02409938.

Ariano, R., 1929. Sulle deformazioni finite della gomma. Rend. Semin. Mat. Fis. Milano 3, 29–52. http://dx.doi.org/10.1007/BF02923477.

Baker, M., Ericksen, J.L., 1954. Inequalities restricting the form of the stress-deformation relations for isotropic elastic solids and reiner rivlin fluids. J. Wash. Acad. Sci. 44 (2), 33–35.

Ball, J.M., 1976. Convexity conditions and existence theorems in nonlinear elasticity. Arch. Ration. Mech. Anal. 63, 337–403. http://dx.doi.org/10.1007/BF00279992.

Batra, R., 1976. Deformation produced by a simple tensile load in an isotropic elastic body. J. Elasticity 6 (1), 109–111. http://dx.doi.org/10.1007/BF00135183.

Beatty, M.F., 1987. Topics in Finite Elasticity: Hyperelasticity of Rubber, Elastomers, and Biological Tissues-With Examples. Appl. Mech. Rev. 40 (12), 1699–1734. http://dx.doi.org/10.1115/1.3149545.

Beatty, M.F., Stalnaker, D.O., 1986. The Poisson function of finite elasticity. J. Appl. Mech. http://dx.doi.org/10.1115/1.3171862.

Blatz, P.J., Ko, W.L., 1962. Application of finite elastic theory to the deformation of rubbery materials. Trans. Soc. Rheol. 6 (1), 223–251. http://dx.doi.org/10.1122/1.548937.

Carroll, M., 2009. On isotropic constraints. Int. J. Eng. Sci. 47 (11–12), 1142–1148. http://dx.doi.org/10.1016/j.ijengsci.2008.10.004.

Chen, M., Tan, Y., Wang, B., 2012. General invariant representations of the constitutive equations for isotropic nonlinearly elastic materials. Int. J. Solids Struct. 49 (2), 318–327. http://dx.doi.org/10.1016/j.ijsolstr.2011.10.008.

Ciarlet, P.G., 1988. Three-Dimensional Elasticity. Elsevier.

Coleman, B.D., Noll, W., 1959. On the thermostatics of continuous media. Arch. Ration. Mech. Anal. 4, 97–128. http://dx.doi.org/10.1007/978-3-642-65817-4_4.

Criscione, J.C., 2004. Rivlin's representation formula is ill-conceived for the determination of response functions via biaxial testing. In: The Rational Spirit in Modern Continuum Mechanics: Essays and Papers Dedicated to the Memory of Clifford Ambrose Truesdell III. Springer, pp. 197–215. http://dx.doi.org/10.1007/1-4020-2308-1_15.

Criscione, J.C., Humphrey, J.D., Douglas, A.S., Hunter, W.C., 2000. An invariant basis for natural strain which yields orthogonal stress response terms in isotropic hyperelasticity. J. Mech. Phys. Solids 48 (12), 2445–2465. http://dx.doi.org/10.1016/S0022-5096(00)00023-5.

Currie, P.K., 2004. The attainable region of strain-invariant space for elastic materials. Int. J. Non-Linear Mech. 39 (5), 833–842. http://dx.doi.org/10.1016/S0020-7462(03)00059-3.

Dal, H., Denli, F.A., Açan, A.K., Kaliske, M., 2023. Data-driven hyperelasticity, Part I: A canonical isotropic formulation for rubberlike materials. J. Mech. Phys. Solids 179, 105381. http://dx.doi.org/10.1016/j.jmps.2023.105381.

Destrade, M., Saccomandi, G., Sgura, I., 2017. Methodical fitting for mathematical models of rubber-like materials. Proc. R. Soc. A 473 (2198), 20160811. http://dx.doi.org/10.1098/rspa.2016.0811.

Ehlers, W., Eipper, G., 1998. The simple tension problem at large volumetric strains computed from finite hyperelastic material laws. Acta Mech. 130 (1–2), 17–27. http://dx.doi.org/10.1007/BF01187040.

Falope, F.O., Lanzoni, L., Tarantino, A.M., 2024. Experiments on the finite torsion of nearly incompressible rubber-like materials: nonlinear effects, analytic modeling and rubber characterization. Int. J. Eng. Sci..

Fitzgerald, J.E., 1980. A tensorial Hencky measure of strain and strain rate for finite deformations. J. Appl. Phys. 51 (10), 5111–5115. http://dx.doi.org/10.1063/1.327428.

Gent, A.N., Thomas, A., 1958. Forms for the stored (strain) energy function for vulcanized rubber. J. Polym. Sci. 28 (118), 625–628. http://dx.doi.org/10.1002/pol.1958.1202811814.

Hill, R., 1968. On constitutive inequalities for simple materials - I. J. Mech. Phys. Solids 16 (4), 229–242. http://dx.doi.org/10.1016/0022-5096(68)90031-8.

Hill, R., 1970. Constitutive inequalities for isotropic elastic solids under finite strain. Proc. R. Soc. A 314 (1519), 457–472. http://dx.doi.org/10.1098/rspa.1970.0018.

Hooke, R., 1678. Depotentia resitutitiva or of spring: Explaining the power of spring bodies. In: Collections. Royal Society, London, pp. 1–67.

Horgan, C.O., Smayda, M.G., 2012. The importance of the second strain invariant in the constitutive modeling of elastomers and soft biomaterials. Mech. Mater. 51, 43–52. http://dx.doi.org/10.1016/j.mechmat.2012.03.007.

Jones, D., Treloar, L., 1975. The properties of rubber in pure homogeneous strain. J. Phys. D: Appl. Phys. 8 (11), 1285. http://dx.doi.org/10.1088/0022-3727/8/11/007.

Kulwant, V., Arvind, K., Prasad, D., Sreejith, P., Mohankumar, K., Kannan, K., 2023. A semi-analytical inverse method to obtain the hyperelastic potential using experimental data. J. Mech. Phys. Solids 181, 105431. http://dx.doi.org/10.1016/j.jmps.2023.105431.

Lainé, E., Vallée, C., Fortuné, D., 1999. Nonlinear isotropic constitutive laws: choice of the three invariants, convex potentials and constitutive inequalities. Int. J. Eng. Sci. 37 (15), 1927–1941. http://dx.doi.org/10.1016/S0020-7225(99)00006-3.

Mihai, L.A., Goriely, A., 2011. Positive or negative Poynting effect? The role of adscititious inequalities in hyperelastic materials. Proc. R. Soc. A 467 (2136), 3633–3646. http://dx.doi.org/10.1098/rspa.2011.0281.

Mihai, L.A., Goriely, A., 2013. Numerical simulation of shear and the Poynting effects by the finite element method: an application of the generalised empirical inequalities in non-linear elasticity. Int. J. Non-Linear Mech. 49, 1–14. http://dx.doi.org/10.1016/j.ijnonlinmec.2012.09.001.

Ogden, R., 1970. Compressible isotropic elastic solids under finite strain-constitutive inequalities. Quart. J. Mech. Appl. Math. 23 (4), 457–468. http://dx.doi.org/10.1093/qjmam/23.4.457.

Ogden, R.W., 1977. Inequalities associated with the inversion of elastic stress-deformation relations and their implications. Math. Proc. Cambridge Philos. Soc. 81 (2), 313–324. http://dx.doi.org/10.1017/S030500410005338X.

Ogden, R.W., Saccomandi, G., Sgura, I., 2004. Fitting hyperelastic models to experimental data. Comput. Mech. 34, 484–502. http://dx.doi.org/10.1007/s00466-004-0593-y.

Pelliciari, M., Sirotti, S., Tarantino, A.M., 2023. A strain energy function for large deformations of compressible elastomers. J. Mech. Phys. Solids 176, http://dx.doi.org/10.1016/j.jmps.2023.105308.

Prasad, D., Kannan, K., 2020. An analysis driven construction of distortional-mode-dependent and Hill-Stable elastic potential with application to human brain tissue. J. Mech. Phys. Solids 134, 103752. http://dx.doi.org/10.1016/j.jmps.2019.103752.

Rivlin, R., Ericksen, J., 1955. Stress-deformation relations for isotropic materials. J. Ration. Mech. Anal. 4, 323–425. http://dx.doi.org/10.1007/978-1-4612-2416-7_61.

Rivlin, R.S., Saunders, 1951. Large elastic deformations of isotropic materials VII. Experiments on the deformation of rubber. Philos. Trans. R. Soc. Lond. Ser. A Math. Phys. Eng. Sci. 243 (865), 251–288. http://dx.doi.org/10.1098/rsta.1951.0004.

Saccomandi, G., 2024. Il problema centrale della teoria dell'elasticità non-lineare secondo signorini. Matematica, Cultura e Società - Rivista dell'Unione Matematica Italiana 9 (1).

Saccomandi, G., Vianello, M.S., 2024. Antonio Signorini and the proto-history of the non-linear theory of elasticity. Arch. Hist. Exact Sci. 78 (4), 375–400. http://dx.doi.org/10.1007/s00407-024-00328-2.

Signorini, A., 1930. Sulle deformazioni termoelastiche finite. In: Proc. 3rd Int. Congr. Appl. Mech. 2, 8G-89.

Signorini, A., 1959. Questioni di elasticità non linearizzata. Rendiconti di Matematica e delle sue applicazioni 18 (5), 95–139.

Thiel, C., Voss, J., Martin, R.J., Neff, P., 2019. Do we need Truesdell's empirical inequalities? On the coaxiality of stress and stretch. Int. J. Non-Linear Mech. 112, 106–116. http://dx.doi.org/10.1016/j.ijnonlinmec.2019.02.004.

Tikenoğulları, O.Z., Açan, A.K., Kuhl, E., Dal, H., 2023. Data-driven hyperelasticity, Part II: A canonical framework for anisotropic soft biological tissues. J. Mech. Phys. Solids 181, 105453. http://dx.doi.org/10.1016/j.jmps.2023.105453.

Truesdell, C., 1952. The mechanical foundations of elasticity and fluid dynamics. J. Ration. Mech. Anal. 1, 125–300.

Truesdell, C., 1956. Das ungelöste hauptproblem der endlichen elastizitätstheorie. ZAMM Z. Angew. Math. Mech. 36 (3–4), 97–103. http://dx.doi.org/10.1002/zamm.19560360304.

Truesdell, C., Noll, W., 1966. The Non-Linear Field Theories of Mechanics. Springer.